Norwegian University
of Life Sciences

Master's Thesis 2022 30 ECTS
Faculty of Science and Technology

Case Study. The Prospect of Using Nature-Derived Chemicals for Removing Metals from Acid Mine Drainage in Folldal, Norway.

Noor al-Huda Sabah Shineshil al-Bedani
Water and Environmental Technology

But it seems reasonable to believe — and I do believe — that the more clearly we can focus our attention on the wonders and realities of the universe about us, the less taste we shall have for the destruction of our race.

Rachel Louise Carson (1907–1964)
Marine biologist, writer, and conservationist

Acknowledgements

This thesis, written at the Faculty of Science and Technology, completes the five year study program of Water and Environmental Technology at the Norwegian University of Life Science (NMBU). The main supervisor have been dr. Zakhar Maletskyi (NMBU), co-supervisors are dr. Agnieszka Cuprys (NMBU), prof. Volodymyr Tarabara (MSU) and prof. Harsha Ratnaweera (NMBU).

I would like to thank dr. Zakhar Maletskyi for guiding and advising throughout the whole period. Thanks to dr. Agnieszka Cuprys for helpful inputs from start to end, for helping with the experiments and answering my many questions.

I would also like to express my gratitude to prof. Volodymyr Tarabara (MSU) and prof. Harsha Ratnaweera (NMBU) for their helpful inputs, and to Lena Oksdøl Foseid for assisting with laboratory preparations and ICP-MS analysis. I am thankful towards Stine Bendigsten from Teta vannrensing AS for providing nature-derived chemicals to the experiments and for sharing valuable experience from previous use.

Ås, June, 2022

Noor al-Bedani

Summary

Folla is one of Norway's most affected rivers by acid mine drainage today. Acidic water with a high concentration of metals is formed during pyrite oxidation in the spoil masses from Folldal Mines in Folldal centre, discharging into Folla and making it inhabitable for aquatic life.

After many years of investigation of different solutions to the problem, The Directorate of Mining proposed a three-step solution in early 2022. One of the solutions proposed is the active treatment of AMD.

This study investigates the use of nature-derived chemicals to remove metals from AMD. Samples were first collected for preliminary tests. Later was chitosan, a biopolymer, used in experiments with model water based on results from the preliminary tests. Chitosan was used as a primary coagulant and as an adsorbent after being modified with biochar to chitosan-covered biochar.

AMD was collected a second time for adsorption batch tests with chitosan-covered biochar and jar tests with NaOH and chitosan as flocculant aid.

The results show that the chitosan-covered biochar removed 99.76% of Cu, 99.83% of Al, 97.88% of Zn, and 99.99% of Fe in the acidic model water, while only removing Fe (93.54%) and Cr (53.57%) in the collected AMD. Chitosan did not remove any metal as a primary coagulant. Chitosan as a flocculant aid did not disrupt the removal of metals through conventional methods; an increase in the sludge volume was observed. Further research is needed to investigate the use of chitosan-covered biochar and chitosan as flocculant aid.

Table of Contents

List of Figures

List of Tables

List of Acronyms

AMD	Acid Mine Drainage
CH-B	Chitosan-covered biochar
DMF	The Directorate of Mining (*Direktoratet for mineralforvaltning med Bergmesteren for Svalbard*)
ICP-MS	Inductively coupled plasma mass spectrometry
MD	The Norwegian Environment Agency (*Miljødirektoratet*)
NFD	Ministry of Trade, Industry and Fisheries (*Nærings- og fiskeridepartementet*)
SFT	Norwegian Pollution Control Authority (*Statens Forurensningstilsyn*)
TDS	Total Dissolved Solids
TSS	Total Suspended Solids

1. Background and Objectives

1.1 Problem Context

While vital to our development, the mining industry brings numerous environmental issues. Acid mine drainage (AMD) is one of the issues stemming from the mining industry, which causes problems and pollutes local environments in many countries worldwide. In several cases, active treatment of the acidic water with chemicals has been implemented as a solution to the problem (Akcil and Koldas, 2006). However, some downsides often appear in the cost of chemicals, sludge production and treatment, and effectivity (Johnson and Hallberg, 2005; Kefeni et al., 2017). Chemicals deriving from nature are biodegradable, non-toxic and often sourced from waste, contributing to a circular economy. One type of nature-derived chemical is chitosan, with early research indicating a great potential in metal removal (Kim and Park, 2021).

In Norway, have mines existed for centuries, with the mining industry becoming an essential part of the national trade in the early 17th century (Gvein et al., n.d.). Active mines are mainly producing minerals for industry and gravel. Meanwhile, metal mines have mostly been abandoned or discontinued (Norges geologiske undersøkelse, 2014; Gvein et al., n.d.). The environmental issues derived from the industry (especially pollution of rivers) came into public awareness in the 70- and 80s. The job to reduce the impact was initiated at most mine sites (Statens forurensningstilsyn, 1992).

One of the most affected rivers is Folla. Folla runs through the village of Folldal (location in Figure 1.1) and is in a very bad ecological and chemical state, with nearly no fish found from Folldal centre and 10-12 kilometres downstream (Knutzen et al., 1986; Løvdal, 2016; Manstad-Hulaas, 2018; Tuttle and Simonsen, 2019, 2020; Evensen, 2021; Evensen and Simonsen, 2022). There have previously been mining activities in Folldal, which have left a visible impact on the environment in and around the village. AMD with extremely high levels of copper and other metals is continuously discharged into the river and will most likely continue to do so if no action is taken (Pabst and Kvennås, 2014). After decades of evaluating possible solutions and options, an action plan was presented in early 2022 by The Directorate of Mining (DMF, *Direktoratet for*

Figure 1.1: Folldal (red pin) is a village in a mountainous area north in Innlandet county, Norway. Map cropped from ©norgeskart.no.

mineralforvaltning). A three-step plan was proposed and estimated to be finished by 2026 (Direktoratet for mineralforvaltning ved Bergmesteren i Svalbard, 2022). The final proposal includes active treatment of the AMD with several conventional chemicals mentioned as examples. This thesis will investigate the prospect of nature-derived chemicals like chitosan being a full-fledged option to the conventional chemicals commonly used.

1.2 Case Study - Folldal Mines

In the village of Folldal in the municipality of Folldal, Innlandet county, Norway, mining activity occurred between 1748 and 1993. Throughout the history, different mining companies have managed the mining industry in Folldal, the last company to do so was Folldal A/S (Stiftelsen Folldal Gruver, n.d.). In total there were five mines in Folldal (see Figure 1.2): the Main Mine (*Hovedgruva*), Northern Geitryggen (*Nordre Geitryggen*),

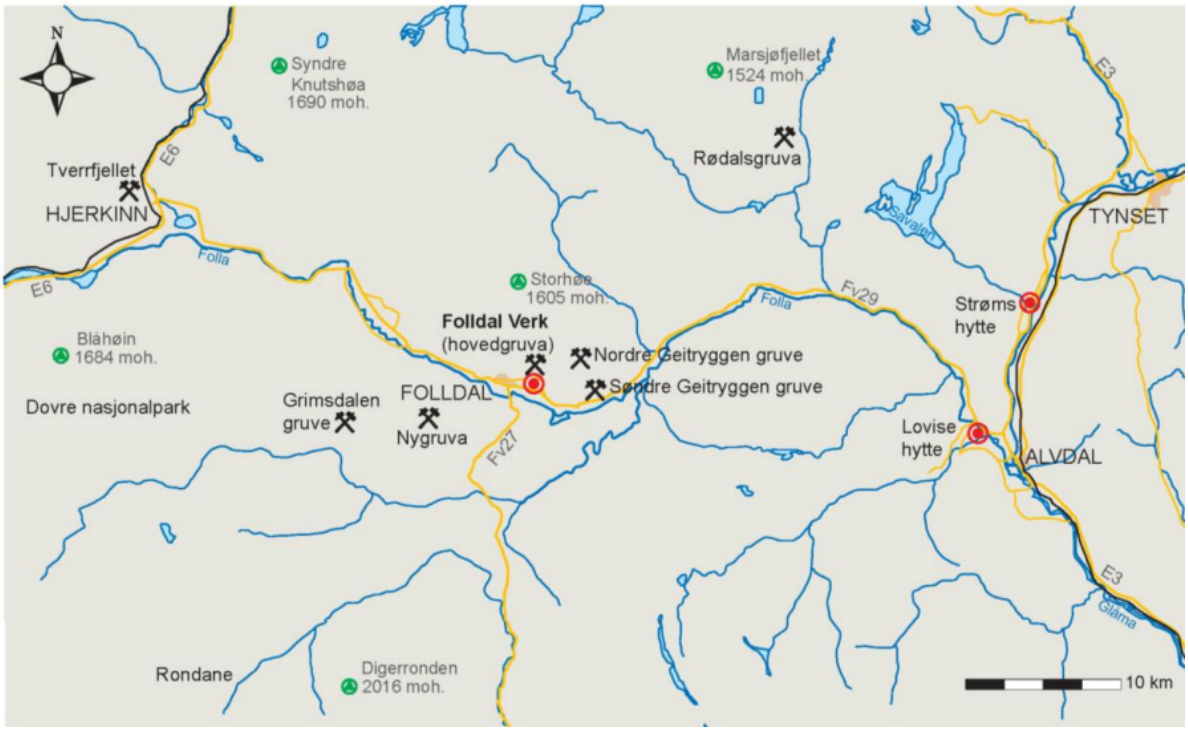

Figure 1.2: Folldal mines (*Folldal Verk*, one of three red markers) and nearby mines (marked with two hammers). The red markers indicate locations for other mine-related activities (for example extracting metals from the mined minerals). Nearby mountain tops are marked with green and named together with their height (meter above sea level, *moh.*). Bigger roads are marked with yellow, and water bodies with blue. Illustration from *Bergverk i Norge - Kulturminner og Historie* (Sæland et al., 2016). Adapted with permission from Fagbokforlaget.

Southern Geitryggen (*Søndre Geitryggen*), the New Mine (*Nygruva*), and the mine of Grimsdal (*Grimsdals Gruve*). Folldal Verk A/S also operated the mine (Tverrfjellet) in the neighbour village Hjerkinn from 1964 until 1993, when the company discontinued its last mine. The mining area in Folldal is now **owned by** the Ministry of Trade, Industry and Fisheries (NFD, *Nærings- og fiskeridepartementet*) after it was escheated in 1990 (Direktoratet for mineralforvaltning med Bergmesteren for Svalbard, 2015).

The mined ore was used to produce mainly copper, zinc, lead, and sulphur. Around four million tonnes of ore were extracted in total in Folldal, while fifteen million tonnes were extracted from Hjerkinn (Stiftelsen Folldal Gruver, n.d.). The spoil from the production was disposed of in general around Folldal centre, which is built around the Main Mine (Pabst and Kvennås, 2014). Besides a museum on the ground level of the Main Mine, the mines are not in use and have been closed off and flooded.

In 1992 the Norwegian Pollution Control Authority (*Statens Forurensningstilsyn*, SFT, now *Miljødirektoratet*, MD) prepared an action plan to clean up old landfills, polluted ground, and contaminated sediments/soil. The action plan included abandoned and discontinued mining sites. One goal in the action plan was to reduce runoff from the

major mines containing copper and zinc by 60-90% by 1995 (Statens forurensningstilsyn, 1992). Folla and the belonging river system was recognized as one of the most affected river systems by AMD in Norway (Statens forurensningstilsyn, 1992).

Parts of the spoil masses were in 1992-1994 removed and disposed of in the then-newly shutdown mine in Hjerkinn (Statens forurensningstilsyn, 1992). However, by 2000 it was recognized that these measures had not improved the situation and that more measures were needed if the goals set by the action plan in 1992 were to be reached (Iversen, 2000; Iversen and Arnesen, 2003). As the landowner, NFD is responsible for the pollution caused by the discontinued mines in Folldal (Direktoratet for mineralforvaltning med Bergmesteren for Svalbard, 2015). In 2003, SFT ordered NFD to implement remediating solutions to the pollution from Folldal mines within 2010 (Folldal kommune, 2021). The orders included the goals:

- Reducing annual discharge of copper from the mining area in Folldal centre into Folla with 60-90 % of the mapped discharge in 1998. The reduction equals 2-8 tonnes of copper yearly, down from 15-20 tonnes of Cu annually .
- Annual average of copper concentration in Folla at Folshaugmoen, 10 km downstream from the discharge point, is reduced to 10-15 µg/L.

Copper is the main target for removal due to its toxicity in aquatic environments (Knutzen et al., 1986; Evangelou, 1998; Amacher et al., 1993). A sampling station at Folshaugmoen was installed in 1966 to monitor the effect on Folla from upstream then-active mines. Folshaugmoen is located around 10-12 kilometres downstream from the AMD discharge into Folla and a couple of kilometers before the river Grimsa is discharged into Folla, diluting the river (Iversen, 2000).

1.2.1 Measures and action

On behalf of NFD, DMF has had the responsibility since 2003 to find a proper solution to the pollution situation by the mines in Folldal (Okkenhaug et al., 2015). Since then have DMF built and improved a trench system to collect AMD from spoil masses in Folldal centre, and tested and evaluated different treatment and remediation technologies for AMD.

January 2022, DMF delivered a final comprehensive action plan to handle/remediate the pollution from the mine site. All parts of the plan must be completed and so in order to realize the order from MD. The proposed solutions are (Direktoratet for mineralforvaltning ved Bergmesteren i Svalbard, 2022):

1. Improving the trench system currently in place. This will ensure minimal 'clean'

water in the system and divert surface water away from the spoil masses and 'pollution'.

2. Covering parts of the spoil masses without compromising the ongoing conservation efforts. This is not MD's desired solution and is unwelcome by the local authorities. DMF mentions several areas with acid-producing potential to be covered up potentially.

3. A treatment plant for treating the AMD collected in the trench system. Based on reports ordered by DMF (Direktoratet for mineralforvaltning ved Bergmesteren i Svalbard, 2022), active water treatment is the most optimal.

The two first steps are estimated to cost 70 MNOK and are likely to be finished within 2024. The third step is estimated to cost 150 MNOK and is expected to be finished by 2026.

Source control and prevention are crucial to reducing AMD produced (Johnson and Hallberg, 2005), which the two first steps cover. By diverting surface water away from spoil masses, the volume of AMD is reduced. This will also ensure less volume needing treatment, and so avoid treating clean surface water.

The second step will cut off the spoil masses from all surface water and stop the pyrite oxidation from producing the AMD. Spoil masses will be wholly or partly covered. However, due to the importance of Folldal mines as a cultural heritage, MD have continuously stated that a treatment solution is preferred over covering or removing spoil masses (Okkenhaug et al., 2015). The local authorities also share this sentiment (Folldal kommune, 2021; Løkken, 2022b,a). It is complicated by the ongoing process from The Directorate for Cultural Heritage to protect the Main Mine and belonging area, including the spoil heaps and other infrastructure (Folldal kommune, 2021).

The third step focuses on AMD remediation. AMD remediation can be achieved either through passive treatment or active treatment. DMF has concluded that active treatment is the most optimal way for AMD remediation in Folldal. The metals are removed by increasing the pH by adding neutralizing chemicals to a point where the metals precipitate. The other technologies tested or evaluated have been unsuccessful or deemed unfit for different reasons. Factors like the local topography and climate might make solutions implemented elsewhere inadequate in Folldal (Direktoratet for mineralforvaltning ved Bergmesteren i Svalbard, 2022; Okkenhaug et al., 2015; Johnson and Hallberg, 2005).

1.3 Acid Mine Drainage

Acid Mine Drainage (AMD, also called Abandoned Mine Drainage or Acid Rock Drainage) is very acidic water with high metal and sulphate concentrations. When sulphide minerals such as pyrite (FeS_2) are exposed to aerobic conditions and water, chemical processes are initiated with the result of forming AMD. The process can occur in natural rock formations, but usually, AMD is a consequence of anthropogenic activities (Evangelou, 1998). AMD is often a significant issue related to abandoned and discontinued mines, as active mines might have a system to avoid production disruption (Johnson and Hallberg, 2005). The chemical reactions leading to pyrite oxidation and AMD formation are (Stumm and Morgan, 1995; Evangelou, 1998):

$$2\,FeS_2 + 7\,O_2 + 2\,H_2O \longrightarrow 2\,Fe^{2+} + 4\,{SO_4}^{2-} + 4\,H^+ \tag{1.1}$$

$$4\,Fe^{2+} + O_2 + 4\,H^+ \longrightarrow 4\,Fe^{3+} + 2\,H_2O \tag{1.2}$$

$$Fe^{3+} + 3\,H_2O \longrightarrow Fe(OH)_3(s) + 3\,H^+ \tag{1.3}$$

$$FeS_2 + 14\,Fe^{3+} + 8\,H_2O \longrightarrow 15\,Fe^{2+} + 2\,{SO_4}^{2-} + 16\,H^+ \tag{1.4}$$

Reaction 1.1 shows the release of acid and the formation of Fe^{2+} through the oxidation of pyrite with O_2. O_2 then oxidizes Fe^{2+} to Fe^{3+} in reaction 1.2. Fe^{3+} precipitates as $Fe(OH)_3$ as seen in reaction 1.3 when pH is between 2.3 and 3.5, releasing more acid into the environment. Any Fe^{3+} that did not precipitate through reaction 1.3 can oxidize additional pyrite and release more acid as in reaction 1.4. Reaction 1.3 is a major contributor to releasing acid into the environment (Evangelou, 1998).

The presence of acidophilic, iron-oxidizing microorganisms like *Acidithiobacillus ferrooxidans*, which can oxidize Fe^{2+}, metal sulphides and S^0, will accelerate the process of pyrite oxidation. Reaction 1.2 is the rate-determining step in lower pH values; *Acidithiobacillus ferrooxidans* can accelerate it by a factor of 10^6 through oxidizing Fe^{2+} (Stumm and Morgan, 1995; Evangelou, 1998; Johnson, 2003).

The four reactions summarize the oxidation of pyrite and, in the process, the release of acid into the environment. The now acidic medium and Fe^{3+} lead to further oxidation of other sulphide minerals. The result is AMD with high content of metals and acid.

Numerous concerns are related to the presence of AMD, such as public health, environmental, and aesthetic issues (Simate and Ndlovu, 2014). In Folldal is the environmental issues stemming from AMD in focus, more specific, the toxic levels of copper in Folla. The three metals are causing ecological damage, can accumulate (Cd only) and therefore are also a concern for health and recreation abilities (Knutzen et al., 1986). It is

essential to note the economic value of having a river with fish for small communities like Folldal. The local authorities estimate that the local community have missed out on four MNOK in turnover since 2010, when the initial goals set by MD were supposed to be reached (Folldal kommune, 2021).

Table 1.1: Annual average concentration from 2017 to 2021 of monitored metals at a reference point upstream Folldal centre, in the AMD, and at Folshaugmoen 10 km downstream. Based on the annual reports made for DMF (Manstad-Hulaas, 2018; Tuttle and Simonsen, 2019, 2020; Evensen, 2021; Evensen and Simonsen, 2022)

Element		Point of reference	Folldal centre	Folshaugmoen
Cu	µg/L	2.43	64967**	20.63**
Zn	µg/L	5.64	42666**	37.48*
Cd	µg/L	0.04	141**	0.1
Al	µg/L	14.80	190541	40.54
Pb	µg/L	0.18	4.21	0.18
Hg	µg/L	0.02	0.014	0.02
Cr	µg/L	0.43	441**	0.43
As	µg/L	0.40	16.68*	0.4
Ni	µg/L	0.94	594**	1.3
Fe	µg/L	47.63	866693	143

***Classified as very bad by MD, causing extensive toxic effects.*
**Classified as bad by MD, causing acute toxic effects. Table A.1.*

The pollution situation caused by AMD is annually monitored by DMF, controlling the ecological and chemical state of Folla (Direktoratet for mineralforvaltning med Bergmesteren for Svalbard, 2015). The AMD in Folldal has an average pH of 2.5, with the average concentration of certain metals of concern seen in Table 1.1. The average annual concentration of AMD, Folla at Folshaugmoen and a reference point upstream showcase the large volume of metals ending up in the river (Table 1.1). MD has set copper as the main target of removal due to its toxic effects on fish. Toxic levels of Cu have been measured in Folla several times more than 10-12 km downstream from the discharge point. The goal of a maximum 15 µg/l annual average of Cu at Folshaugmoen is still classified as 'bad' (see A), which means it has acute toxic effects. In Folla, the metals Cu, Zn, and Cd are the main problem as they are detected in high dosages at Folshaugmoen. High concentrations of metals have also been periodically observed further downstream from Folshaugmoen and all the way to Glomma (Knutzen et al., 1986; Iversen and Arnesen, 2003).

The primary source of the generation of AMD in Folldal is the spoil masses from the previous mining activities (Pabst and Kvennås, 2014). The dominating form of sulphide mineral in the spoil masses is pyrite (FeS_2), in addition to some chalcopyrite ($CuFeS_2$), sphalerite ((Zn, Fe)S), and naturally occurring sulphur (S^0)(Pabst and Kvennås, 2014).

The masses are heterogeneous (including factors like size, mineral and weathering) and have acidification potential. It is estimated that the masses will continue to oxidize and form AMD for years (maybe hundreds) as it is now. Although it is clear that the metal concentration in Folla originates from AMD from the Main Mine, arbitrary measured high concentrations of some metals have been observed upstream from Folldal. These observations indicate other sources of high background levels of metals, natural or possibly from other older abandoned mines found upstream. However, there is no doubt that the Main Mine is a dominant source of pollution (Evensen, 2021).

There are huge variations in metal concentration not only from day to day but year to year. However, it is seen that within a year, the metal concentration drops during the spring flood and melting of snow in April/May, as seen in Figure 1.3. While the spring flood and snow melting lead to more water rich in oxygen to contribute to the pyrite oxidation, will the general increase of water in Folla and the sampling station at the same period dilute the streams and reduce the metal concentration.

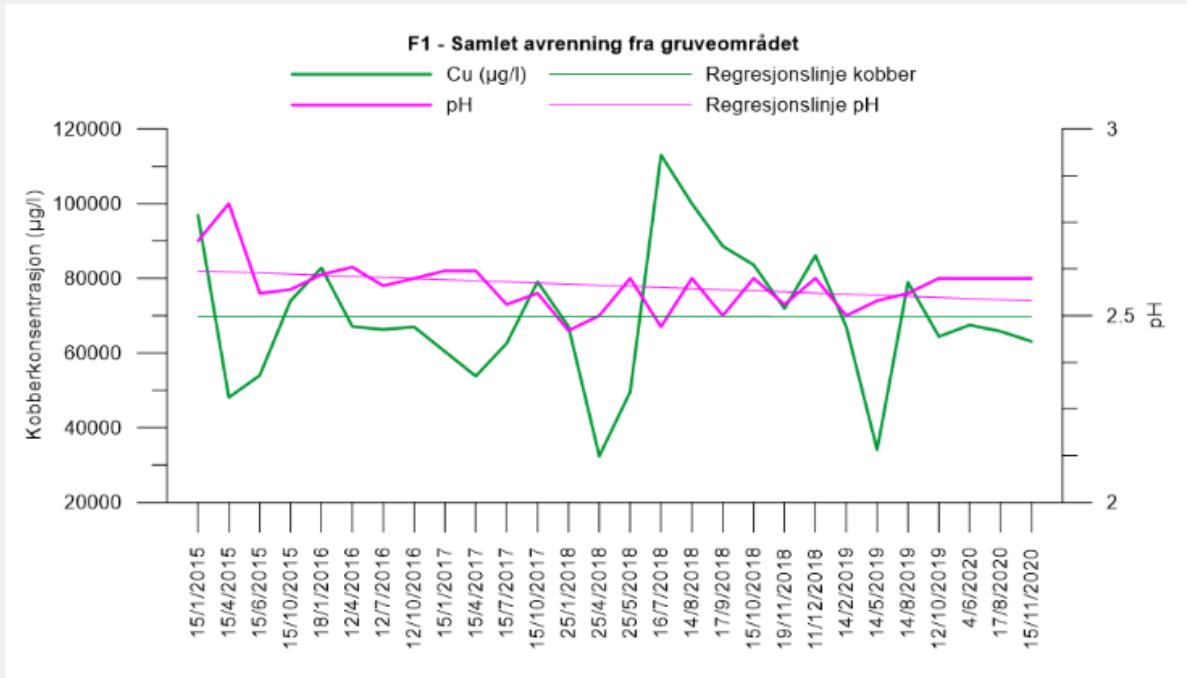

Figure 1.3: The Cu concentration and pH in the AMD from Folldal mines over a period from 2015 to 2020 (Evensen, 2021). Adapted with permission from DMF.

All the spoil masses have acid production potential (Pabst and Kvennås, 2014). While the top layer of spoil masses has been exposed for a while and has reduced acid-producing potential, there is no way to assume how long they will continue to produce acid (and in the process also metals) (Pabst and Kvennås, 2014). The masses below the surfaces are protected from contact with O_2 and the first steps of pyrite oxidation; however, since the pH is below 3.5, there can be oxidation of pyrite through Fe^{3+} in the spoil masses

not in contact with air (Eq. 1.4) (Pabst and Kvennås, 2014).

Copper is highly toxic for many aquatic organisms, including fish (Evangelou, 1998). It does not bioaccumulate but is acute toxic for fish and will make the river inhabitable in high enough concentrations. Zinc is related to the same issues as Cu but is not as toxic. Zn is more of a concern regarding its association with Cd (Knutzen et al., 1986). Aluminium, chromium, and nickel are other metals directly affecting aquatic life (Evangelou, 1998). Chromium can also accumulate in an organism but not further in the food chain (Knutzen et al., 1986).

Cd and Hg are problematic due to their ability to accumulate in an organism and bioaccumulate (Knutzen et al., 1986). Both heavy metals can be stored for several years in organisms and passed to the next organism in the food chain. They become toxic in considerably small dosages, so even minimal levels can be problematic. Although Fe is not directly toxic, the excessively high concentration of Fe discharged into Folla precipitates, causing visible pollution by turning the riverbanks and the river water reddish. The precipitation of all metals when discharged into Folla also leads to sedimentation in the river bottom. While not deemed a direct problem to the ecosystem to consider any action (Okkenhaug et al., 2015), it is not ideal with highly concentrated metals in the river sediments in the future.

1.4 Metal Precipitation of AMD

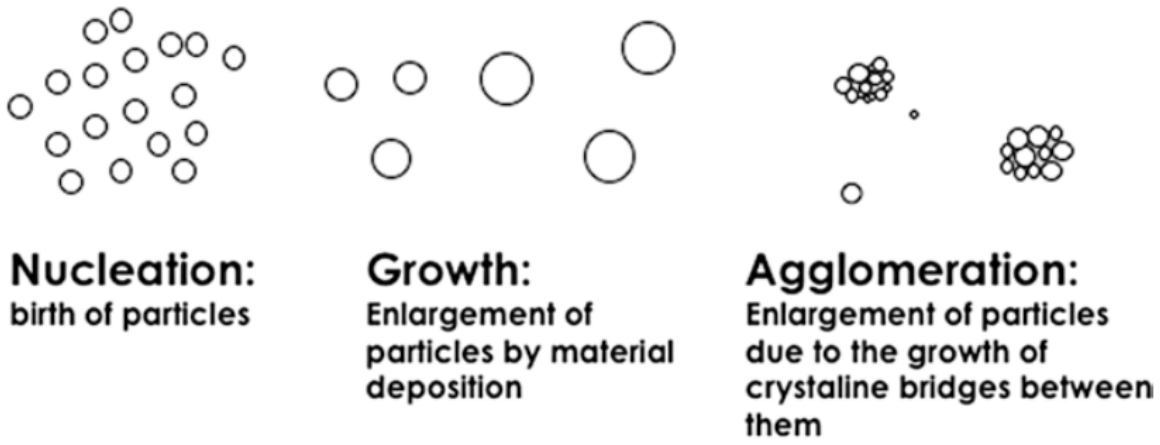

Figure 1.4: An illustrative description of the precipitation mechanisms: nucleation, growth, and agglomeration (Lewis, 2017). Adapted by permission from Springer Nature Customer Service Centre GmbH: Springer Nature. Precipitation of Heavy Metals by Alison Lewis. COPYRIGHT. 2017.

Active treatment of AMD refers to actively adding chemicals to treat the polluted water. The most common mechanism for removing the metals from the water is through

neutralization of the water to the desired pH where the metals precipitate (Evangelou, 1998). The mechanism behind precipitation is described as the compound's solubility in a medium being surpassed (Stumm and Morgan, 1995). The solute concentration is higher than the solid-liquid equilibrium, leading to the precipitation of the compound.

The precipitation goes through three mechanisms, illustrated in Figure 1.4 (Lewis, 2017). First is the initial formation of the solid phase, nucleation, where aggregates of the colloids in a supersaturated solution reach the size where they will grow and not redissolve. Then comes growth, where the particles enlarge due to the accumulation/deposition of other particles on the existing surface. Lastly is agglomeration, where at least two larger particles form a larger floc/particle from colliding and forming crystalline bridges (Lewis, 2017). There are various precipitating agents, such as sulphide precipitation (Lewis, 2017), and active technologies removing metals, such as membranes (Simate and Ndlovu, 2014). The type of precipitation discussed by DMF is hydroxide precipitation; therefore, will the focus be on metal hydroxide precipitation (Direktoratet for mineralforvaltning ved Bergmesteren i Svalbard, 2022).

1.4.1 Hydroxide precipitation

The most used chemical precipitation techniques are metal hydroxide precipitation. The water is neutralized by adding bases such as NaOH, $Mg(OH)_2$, NH_4OH, limestone ($CaCO_3$), hydrated lime ($Ca(OH)_2$) or quicklime (CaO). The results are the precipitation of metal hydroxides (Lewis, 2017; Evangelou, 1998).

While it is easy to implement, relatively cheap and controlled through pH, it is also related to high costs, a large volume of sludge and limited levels of final metal concentration. The sludge formed is gelatinous, and sulphate removal is limited (Lewis, 2017; Rhazi et al., 2001; Johnson and Hallberg, 2005).

Balintova and Petrilakova, 2011, did experiments on selective recovery of metals on AMD with copper, zinc, iron, aluminium, and manganese, and through neutralization with NaOH to pH 8.2 removed over 90% of all the metals besides manganese, which only 15.9% was removed.

1.5 Adsorption

The basis of most surface-chemical processes is adsorption, in which particles accumulate on the solid-water interface. The chemical species may be adsorbed due to electrostatics or by electron sharing to a surface. Adsorption covers several mechanisms, including some of the already mentioned ones. One form of adsorption is through hydrophobic expulsion of hydrophobic substances. Hydrophobic matter in water are compounds not

so soluble in water. When added to water, the matter will avoid water and instead associate with nonpolar surfaces of other particles, accumulating (becoming 'adsorbed') on the surface (Stumm and Morgan, 1995). Examples of nonpolar surfaces can be minerals or organic particles. Some matters with both hydrophobic and hydrophilic parts tend to move towards the surface/interface of the water and self-associate. Most particles have functional groups on their surface. One form of adsorption is surface complexation reaction, where the functional groups form complexes with metal ions

Adsorption is described through adsorption isotherms. The adsorption isotherms show the relationship between the dissolved concentration of the adsorbate and the adsorbed concentration of the adsorbate at constant temperature and pressure. The adsorption isotherms are often described through different models. The two most common models are *the Langmuir Isotherm* and *the Freundlich Isotherm*.

1.6 Flocculation

Coagulation and flocculation are often mentioned together and sometimes interchangeably. Coagulation is the destabilisation of particles by coagulants, enabling the particles to form flocs. Flocculation, the aggregation of the colliding particles, is a physical process following the physicochemical process of coagulation in water treatment (Pivokonský et al., 2022).

To alter floc characteristics like floc size, density, and settleability, to mention a few, flocculant aids are added. Flocculant aids also supplement the flocculation process, with polyelectrolytes being effective in enhancing the flocculation rate/orthokinetic flocculation (Bratby, 2016). Polyelectrolytes are generally viewed as ideal flocculant aids; however, the flocculation mechanism depends on the polyelectrolytes' characteristics.

The flocculation mechanism can roughly be divided/classified between charge neutralization, charge patching, bridging, sweeping, and special interactions. The different mechanisms are roughly explained in Table 1.2. The flocculation mechanism is also influenced by other factors that affect the flocculant and its characteristics. These external factors are flocculant dose, pH, ionic strength and temperature (Yang et al., 2016).

Table 1.2: Overview of the different flocculation mechanisms and a description of the said mechanism.

Mechanism	Description
Simple charge neutralization	Due to the dispersed colloids in wastewater being charged, the resulting electrostatic repulsion effects stop the colloids from aggregating and forming bigger flocs. By adding flocculant aid oppositely charged, the opposite charges 'cancel out', enabling a higher collision frequency between the colloids, and therefore the formation of flocs. If an excess of flocculant dose is added, there will be a re-stabilization effect whereas the dispersed particles are completely surrounded and so the charge will be more than neutralized. Therefore, it is essential when the main flocculation mechanism is charge neutralization to know the optimal dosage of flocculant aid. The zeta potential will quickly approach zero when the optimal dosage is added.
Charge patching	In many cases, there is no dosage where an excess dosage of flocculant leads to the opposite of neutralization. Instead, the colloids adsorb the oppositely charged flocculant to its surface in a heterogeneous coverage. As a result, there will be small regions on the surface of the colloid with different charges. This leads to direct electrostatic attractions between the suspended colloids, and later collisions between them result in larger flocs. If the charge patching is the main mechanism behind the flocculation, the flocculation happens before charge neutralization, opposite of the charge neutralization mechanism.
Bridging flocculation	Bridging flocculation is a mechanism caused by polymers with long-chain conformation. When the colloids adsorb the long-chained polymers to their surface, the rest of the polymer will dangle freely in the water/aquatic medium. More colloids will adsorb along the chain until there are no more dangling ends. A bridge is formed between the particles, aggregating the colloids and making larger flocs. The mechanism behind the adsorption depends on the type of flocculant and can be due to cation exchange, electrostatic linkages, hydrogen bonding or ionic bonding (Bratby, 2016).
Sweeping flocculation	One effect of the use of inorganic coagulants like metal salts is the formation of hydroxide precipitates aggregating into large hydroxide flocs. The hydroxide flocs trap and sweep the colloids in the water. This mechanism is also present in some polymers with limited solubility.
Chelation	Polymer chains normally contain several active functional groups. These groups can chemically react to certain pollutions through specific forces (Yang et al., 2016). In the case of metals (as in AMD), chelation is a process where metal ions bond with chelate groups. The chelating agents must be capable of associating with metal ions. An example of such a group is NH_2 (Evangelou, 1998).

1.7 Chitosan

Several issues of concern have been raised regarding the use of inorganic chemicals in the water treatment industry. Issues include topics like possible health issues from inorganic chemicals to the practical problems arising from using inorganic chemicals. *Chitosan* can be more accessible and even produced by most countries. Sourced from the food industry as a by-product of shrimp and crab consumption, chitosan can also be a way

to turn into a circular economy. Chitosan is a nature-derived, cationic substance made

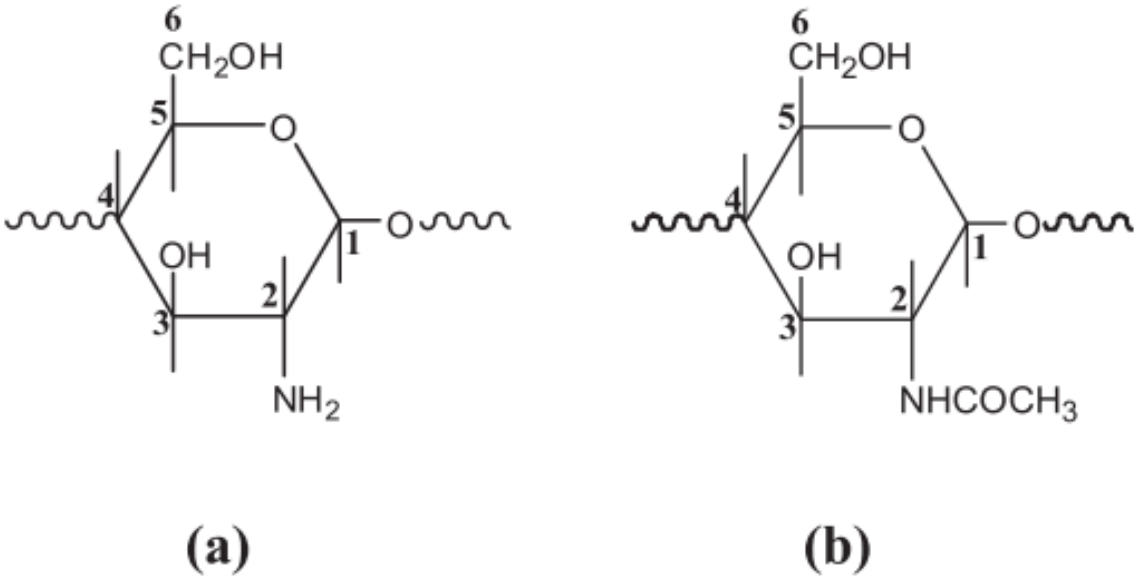

Figure 1.5: Illustration of a) the structure of chitin, and b) the structure of chitosan (Yang et al., 2016). Reprinted from Water Research, Vol 95, 59-89, Copyright (2016), with permission from Elsevier.

from the natural polysaccharide chitin. Chitin is one of the most abundant polymers in the world, only second to cellulose (Rinaudo, 2006). It is produced/synthesized by various organisms worldwide, and the leading source for commercial production is the exoskeleton of crabs and shrimps. Chitosan is a linear copolymer of D-glucosamine and N-acetyl-D-glucosamine, formed when chitin is deacetylated to a degree of around (minimum) 50% (Figure 1.5). The characterisation of chitosan mainly depends on two parameters: the degree of deacetylation and molecular weight. The substitution of acetyl groups in chitin with amino groups gives chitosan various applications and makes chitosan soluble in water.

Due to its characteristics, chitosan is used in multiple fields, including biomedicine, agriculture, cosmetics, food and beverage, biopharmaceutics, and water and waste treatment (Muxika et al., 2017; Rinaudo, 2006). The chemical structure of chitosan opens for designing polymers with particular abilities by specific modification (Brião et al., 2020; Igberase et al., 2018; Markovic et al., 2020; Rinaudo, 2006; Sun et al., 2019). Chitosan is also a cationic polyelectrolyte; when added to an acidic medium, the NH_2 groups will be protonated. Due to these characteristics, chitosan opens to become an optimal flocculant aid (Renault et al., 2009; Yang et al., 2016).

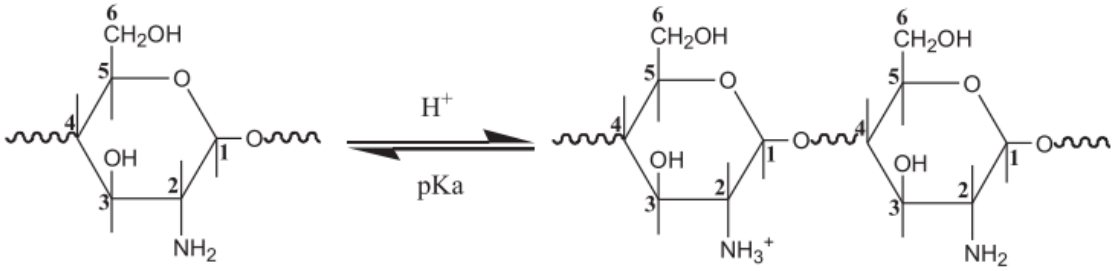

Figure 1.6: The protonation of chitosan (Yang et al., 2016). Reprinted from Water Research, Vol 95, 59-89, Copyright (2016), with permission from Elsevier.

Flocculation mechanisms of chitosan

As previously mentioned, there are different types of mechanisms behind flocculation. The mechanisms are also valid when using chitosan as a flocculant aid. Many of these mechanisms also depend on external factors (as mentioned). For chitosan, this also includes its characteristics and behaviour in the medium. Some of the mentioned characteristics are the degree of deacetylation and molecular weight, which will be more apparent when looking at the different flocculation mechanisms. In general, it can be said that the flocculation efficiency of chitosan increases with lower pH, higher ionic strength in medium, and higher temperatures. The effect of dosage depends on the primary flocculation mechanism (if simple charge neutralization or charge patching is the dominant mechanism). Regarding charge neutralization, the protonation of chitosan (illustrated in Figure 1.6) in an acidic medium allows charge neutralization of negative-charged pollutants. The effect of charge neutralization depends on the distance between two charge units along the polymer chain (the charge density). This comes to the number of amino groups in chitosan. While the number of amino groups depends on the degree of deacetylation, the protonation of chitosan also depends on pH, with the degree of protonation being higher at acidic levels. The ionic strength of the medium might also play a role in the charge density of the chitosan (Yang et al., 2016).

Chelation in chitosan depends on available amino and hydroxyl groups, making chitosan better than other natural compounds to form chelates (Rhazi et al., 2001). When it comes to bridging flocculation with chitosan as flocculant, the mechanism also depends on the degree of deacetylation, pH, and ionic strength. When it comes to the degree of deacetylation, it is difficult to predict the effects it has (Renault et al., 2009; Yang et al., 2016).

1.7.1 Metal removal with chitosan

Several studies have investigated the removal of metals by chitosan, some of which will be swiftly introduced.

Bessho et al., 2019, found that using 0.1 g of chitosan in a water mix of Cu, Zn, and Mn, almost no metal was recovered at pH 2. However, the removal of Cu and Zn increased to nearly 90% and 60% when pH was increased to pH 3. Minimal recovery of Mn was found in the pH range from 2 to 5. The presence of chelating groups like NH_2 and hydroxyl groups in chitosan allows for the chelation of metals (Bessho et al., 2019).

In the work of Sun et al., 2019, several chitosan-based flocculants were used under varying conditions to investigate the removal of Cu, Cr and Ni from model wastewater. The removal mechanism was mainly chelation, charge neutralisation, adsorption bridging, and sweep flocculation (Sun et al., 2019). Cu was removed in a range of 68.2 - 85.1%, Cr in 68.5 - 76.1%, and Ni in a range of 65.4- 75.7%. It was found that different flocculants were optimal for different metals.

Modified chitosan in the form of microspheres was used by Laus et al., 2007, to remove acidity and metals from coal mining wastewater. The results show that the microsphere was able to increase the pH from around 2.5 to almost neutral values and remove Fe^{3+}, Al^{3+} and Cu^{2+} entirely. The increase in pH was due to the protonation of the NH_2 groups. These groups were the main adsorption sites for the metals and a chelating group, forming chelates with the metal ions. The microspheres could also be reused and recycled, suggesting more environmentally friendly than other solutions (Laus et al., 2007).

Gidas et al., 1999, compared the effectiveness of chitosan as a primary coagulant against alum in both municipal and industrial wastewater (siderurgical industry) based on Cu^{2+} removal, turbidity removal and COD. The results show that chitosan is superior to alum in removing copper and turbidity from industrial wastewater while being much less efficient for removal in a mix of bentonite and drinking water. The results showcased the importance of particle types for removal with chitosan. However, it was concluded that the removal was higher with higher pH (Gidas et al., 1999). This conflicts with what was found by Rhazi et al., 2001, where chitosan was found to form complexes with copper ions with the optimal pH range of 5-7 (Rhazi et al., 2001).

While several studies have been made covering the removal of metals with chitosan from wastewater, most of the research is also difficult to compare due to different experimental setups. Kim and Park, 2021, have reviewed the use of biosorbents to treat AMD, including studies with modified chitosan. The review shows promising potential in using chitosan; however, more research is needed in general (Kim and Park, 2021).

Modified chitosan: chitosan-covered biochar

Another type of nature-derived material is biochar, formed through pyrolysis of organic waste. The temperature during the pyrolysis process ranges from 300°C to 900°C. The

organic waste used as feedstock varies, ranging from municipal wastewater sludge and food waste to animal manure and wood chips (Wang and Wang, 2019). The wide range of waste and feedstock used to produce biochar also results in varying properties from feedstock to feedstock and the pyrolysis process and temperature. Depending on these properties, biochar can be used, for example, for soil remediation and water treatment (Wang and Wang, 2019). As with chitosan, biochar can be modified to enhance specific properties.

One form of modification which has been a popular research topic recently is the chitosan-covered biochar (CH-B). The product combines two types of materials coming from waste and has been investigated as nature-derived options for inorganic and synthetic polymers (Gao et al., 2022). Biochar and chitosan are as they are not entirely effective as they potentially can be, but through modification can be adjusted. As mentioned, biochar and chitosan can easily be modified through different methods to enhance specific functions in the chemical (Wang and Wang, 2019).

In the research of Zhou et al., 2013, the removal of Cd, Cu and Pb from water with biochar made of four different feedstock (bamboo, sugarcane bagasse, hickory wood, and peanut hull) were compared with the results from responding CH-B. All the CH-B had higher Cu removal efficiency than the responding biochar. All CH-B besides peanut hull had a higher removal efficiency of Cd. At the same time, only CH-B of bamboo and hickory wood saw a significantly higher removal of Pb. In contrast, CH-B of sugarcane bagasse and peanut hull saw a decrease in removal compared to responding biochar. It suggests that the metal was removed through chelation with the amine functional group (Zhou et al., 2013).

Cuprys et al., 2021 investigated the use of chitosan-covered biochar to remove As, Cd, and Pb, simultaneously with the antibiotic element ciprofloxacin. First was biochar made of different feedstock (pinewood, almond shell, and pig manure), where the one with the highest adsorption capacity (pig manure) was used to make CH-B. The study showed that the feedstock used for biochar influences the removal efficiency and adsorption capacity (Cuprys et al., 2021). CH-B had an increased adsorption capacity for all pollutants besides Pb. CH-B also outperformed biochar and granulated active carbon in simultaneous removal efficiency for all targeted pollutants in real wastewater.

Song et al., 2021, the removal of Cr, Cu, Se, and Pb, from oil sands process water with biochar made of municipal sewage sludge as feedstock was compared to the removal with the corresponding CH-B. The CH-B removed the metals at a high rate and higher than biochar and chitosan alone. Chelation, hydrophobic interactions, electrostatic and chemical adsorption all play a role in removing metals (Song et al., 2021).

1.8 Research questions and knowledge gap

With active treatment of the AMD in Folldal being proposed, the choice of chemicals is now a new issue to discuss. The cost of NaOH, the sludge volume and operating issues with limestone, and the difficulties with sulphides are just a few issues raised with the conventional chemicals used to remove metals from water. Additionally, there is the issue with sludge handling,

Nature-derived chemicals are biodegradable, often non-toxic and can be more accessible, sometimes deriving from different kinds of wastes and contributing to a more circular economy. From mentioned studies, chitosan has removed a wide range of metals in various types of water. This covers different ways to apply chitosan, e.g. as flocculant aid, as a coagulant, as adsorption material and as membranes. The mechanisms behind the removals have been identified as chelation and different adsorption and flocculation mechanisms (Sun et al., 2019; Laus et al., 2007; Bessho et al., 2019). The studies have been conducted with model water based on different wastewater and raw waters like coal mine effluents. However, there is not enough research covering the use of chitosan to remove metals from AMD (Kim and Park, 2021). The range of techniques used to apply chitosan and the different types of wastewater used is diverse but scarce.

This study is foremost preliminary due to the varied but inadequate literature about the removal of metals from AMD with chitosan and modified chitosan. To narrow down which technique and removal mechanism in chitosan is most promising, different techniques should be investigated first.

This paper will primarily investigate the most common application of chitosan for metal removal and if the techniques can be used for removing copper in Folldal. This is being done by narrowing it down to the following research questions:

1. How are novel methods involving nature-derived chemicals such as chitosan and biochar performing compared to conventional treatment methods in removing metals from AMD?

2. Can novel methods involving nature-derived chemicals improve conventional methods' performance for removing metals from AMD?

By answering these research questions, will this thesis work as a preliminary study into the use of chitosan to remove metals from AMD and, more particularly, the possibility of using nature-derived chemicals in the removal process of metals in Folldal.

2. Material and Methods

To examine the use of chitosan for removal of metals from AMD, different experiments were planned to cover various aspects of treatment efficiency and removal technology. The first experiments were undertaken with model water based on the composition of the AMD from Folldal. Therefore, collecting samples and preliminary experiments were completed first. The collected samples were used for preliminary tests at the laboratory at NMBU, to establish metal composition for making model water. Afterwards, experiments with chitosan and model water were performed. Some experiments were first performed at NMBU, while different experiments were performed in MSU, East Lansing, MI, USA. Lastly were experiments conducted at NMBU with AMD collected in Folldal. An overview of what experiments performed where is illustrated in Figure 2.1.

Due to a delay in the ICP-MS results from MSU, the method-section covering that part of the experiments is moved to Appendix C on page 49.

The overall objective is to evaluate the prospect of treatment methods/technologies/techniques involving nature-derived chemicals like chitosan, to remove metals from AMD in Folldal.

2.1 Sampling and composition of AMD

The sampling location (32N N 6889621 E 551005, 2.2) is the same as the location used by DMF to take samples for monitoring the AMD discharge to the river. It is a collection point where the trench system in place directs the water to before discharging it to the river. The collection point is on the floor inside a small shed, covered with a lid.

Samples were collected two times; first time on 07.02.2022 for preliminary analyses of the water composition, second time on 02.05.2022 for final experiments.

The samples were collected with a plastic bucket tied to a rope and poured into pre-prepared containers. On 07.02., samples were collected in bottles; one 1 L amber glass bottle and three 500 mL plastic bottles. Two of the plastic bottles were acidified for

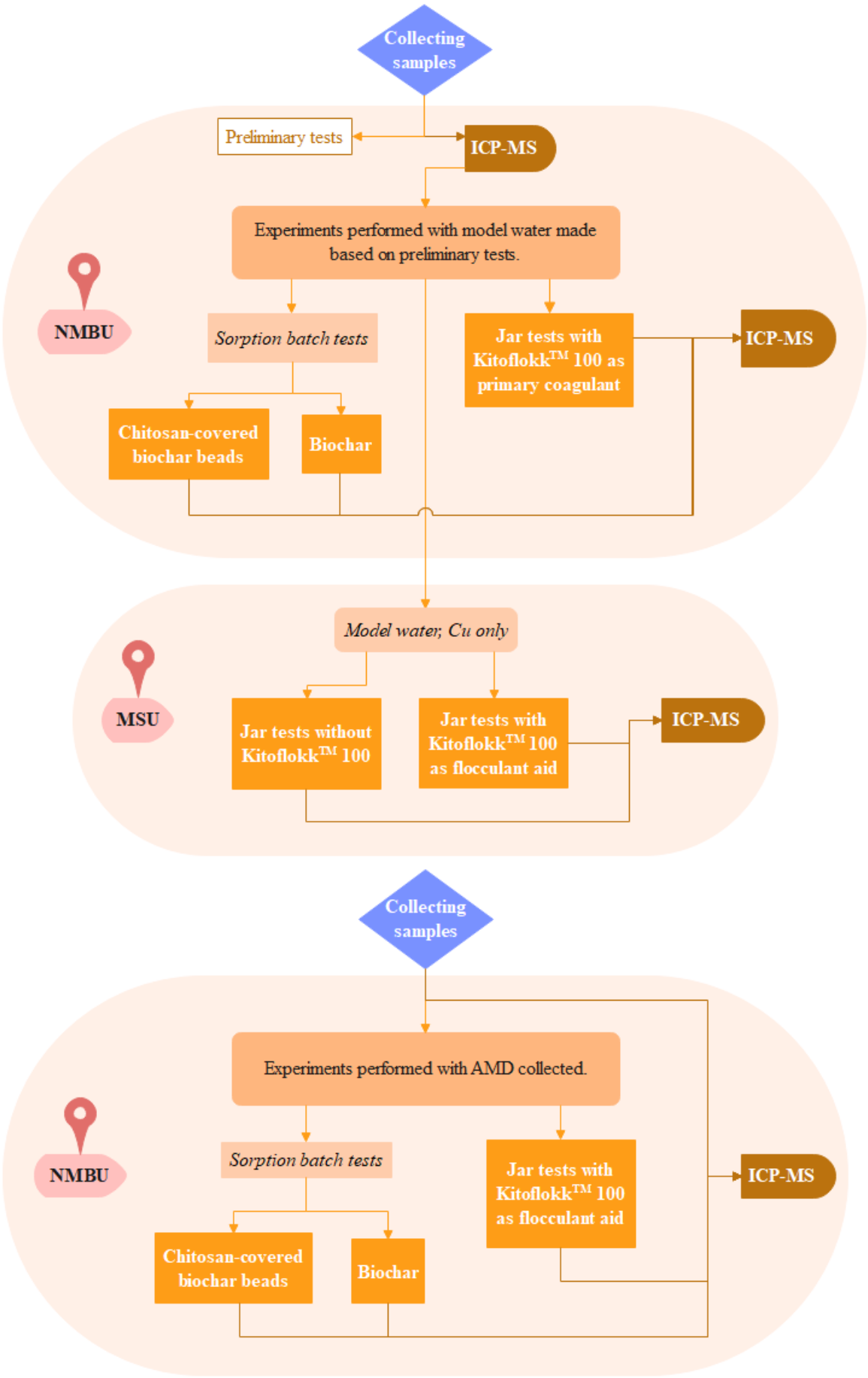

Figure 2.1: A schematic overview showing what experiments was performed and location for experiments.

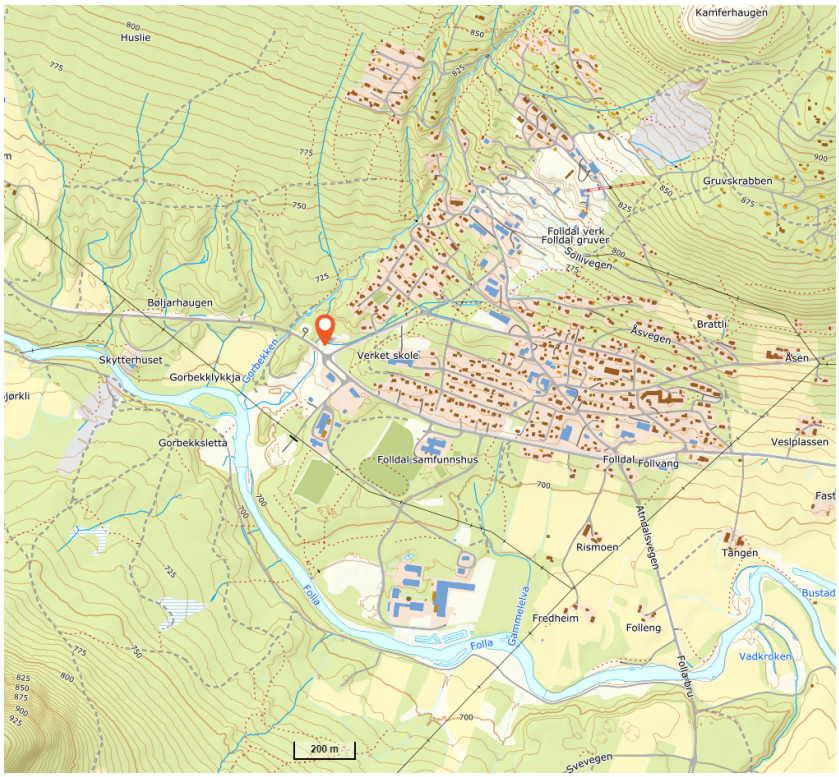

Figure 2.2: The location for sampling, 32N N 6889621 E 551005, is marked with a red pin. Cropped from ©norgeskart.no.

preservation; one with 1 mL of nitric acid, second with 1 mL of sulphuric acid. Conductivity and pH were measured, after calibration of the instruments.

Back in the laboratory at NMBU was TSS, TDS, turbidity, conductivity, and pH, measured while the metal composition of the acidified water was analysed with ICP-MS.

On 02.05., a new, pre-washed 20 L container made of HDPE was filled up and acidified/preserved with pure nitric acid ($\sim$ 1.5%). pH, turbidity, and conductivity were measured on-site after calibrating the instruments, then measured again at NMBU.

2.1.1 Temperature and weather

To properly understand the results from the samples collected is the weather throughout January, February, and April, and the weather seven days prior to sampling dates presented. The data are from seklima.met.no, and The Norwegian Meteorological Institute and their closest weather station, which is Fredheim, Folldal, station number SN9160, location 32N N 6888860 E 551879. The station is located 694 meters over sea level, around 1.5 kilometres from the point of sampling. The climate of Folldal is typical continental climate in a mountainous area in Norway. Cold winters, hot summers, and relatively dry compared with.

Weather and Temperature - 07.02.2022 According to the monthly reports from The Norwegian Meteorological Institute for January and February (Grinde et al., 2022a,b), the period was warmer and wetter than the climate normal (1991-2020) for the same period. In January was the mean temperature 4.3°C over the normal mean temperature, while precipitation was 225% of the normal precipitation. The precipitation, mean, minimum, and maximum temperature for the week before sampling is illustrated in Figure 2.3. It shows that the mean temperature for the period before sampling was below 0°C, with just two days having maximum temperature just over 0°C. Therefore is the precipitation for those days most likely being in the form of snow.

Weather and Temperature - 02.05.2022 According to the monthly report from The Norwegian Meteorological Institute for April (Grinde et al., 2022c), the month was colder and dryer compared with the climate normal. The mean temperature was -0.8°C colder than the mean temperature for the same period in the climate normal. The precipitation was 56% of the normal precipitation. The precipitation, mean, minimum, and maximum temperature for the week before sampling is illustrated in Figure 2.4. It shows that there is nearly no days with precipitation seven days before sampling, and very little for the days with precipitation. The mean temperature is over 0°C, while minimum temperature is below 0°C most days.

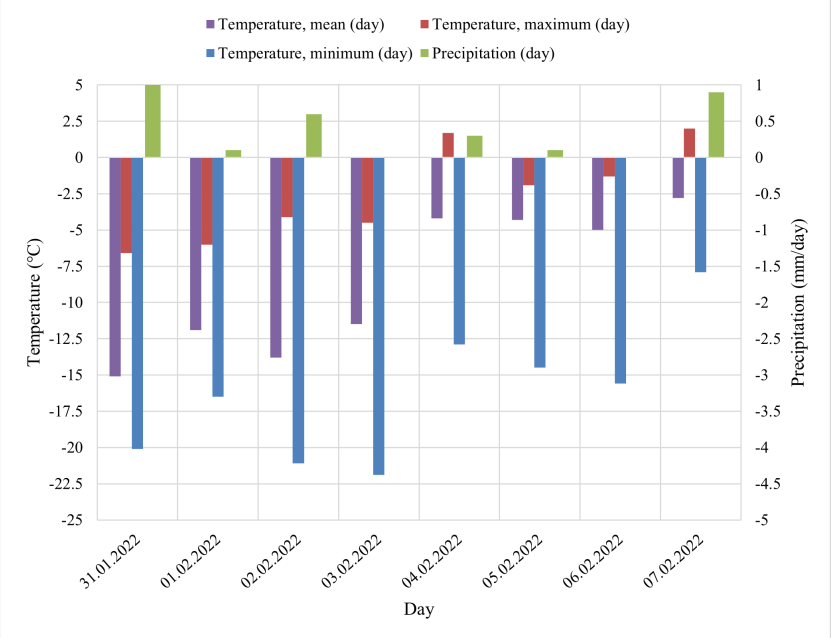

Figure 2.3: Illustration of the mean, maximum, and minimum temperature each day, including total precipitation each day. Covering 31.01.2022 to 07.02.2022, the first day of sampling. Data collected from seklima.met.no.

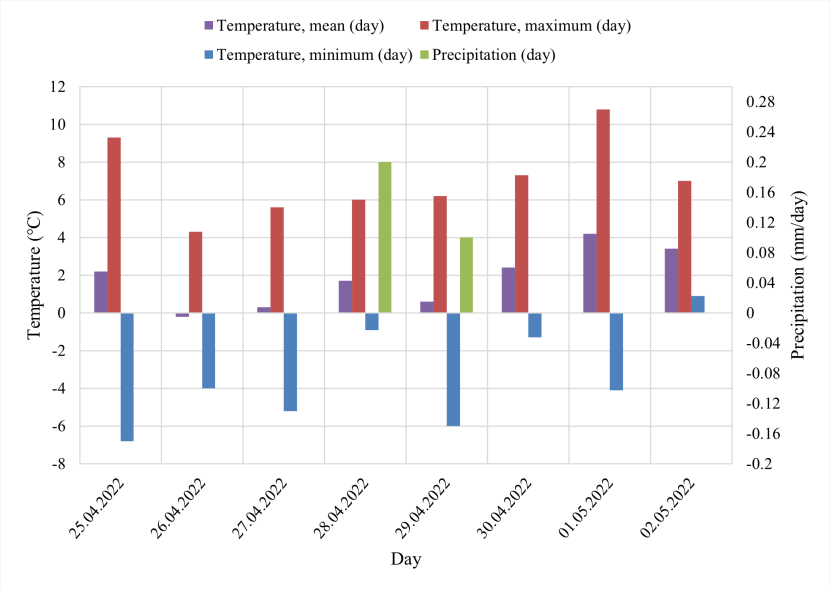

Figure 2.4: Illustration of the mean, maximum, and minimum temperature each day, including total precipitation each day. Covering 25.04.2022 to 02.05.2022, the second time sampling. Data collected from seklima.met.no.

2.2 Parameters

Six different parameters were measured in one or more of the experiments. A short summary of the importance of the parameter and type of equipment used is described under the said parameter.

2.2.1 pH, conductivity, and turbidity

The parameters of pH, conductivity, and turbidity are standard part of water composition and essential for most activities (treatment, consumption, experiments, etc) involving water and to the efficiency of different treatment/removal techniques.

To determine the pH, a pH-meter was used. The pH-meter was calibrated frequently with the standard solutions. For measuring at NMBU and on-site, the pH-meter used was *Model 370* from Jenway.

Conductivity was measured with *WTW Cond 3210*, and turbidity was measured with *Hach 2100Qis Portable Turbidimeter*, which was calibrated before used. Conductivity gives an indication of the ions in the water. Turbidity is used as an indication of particles in water based on the turbid.

2.2.2 TSS and TDS

Total Suspended Solids (TSS) are the particles with a size of two micrometres (micron) or more, while Total Dissolved Solids (TDS) are the dissolved substances under two micrometres. TSS gives the weight of suspended particles in the medium and is used as a quality parameter. The TDS gives an indication of the dissolved particles in the medium, including metals and other ions.

The method used to measure TSS and TDS is the same as described by American Public Health Association et al., 2012. This method uses the weight difference of a filter before, and after filtration and heating at 105°C, to find TSS in the sample. To find TDS, the filtrate from TSS was also heated at 105°C. More information about the biochar can be found in Cuprys et al., 2021.

2.2.3 Metals

The metal composition of the water is the major parameter in this case study. Inductively coupled plasma mass spectrometry (ICP-MS) can detect very low concentration of elements. The elements are ionized as they pass through a plasma source. The ions are then sorted based on their mass.

The samples were filtered and acidified with HNO_3 before being delivered to the operator of the instrument for further preparing and analysing. For the analyses of the experiments with AMD, the samples were centrifuged with *Centrifuge 5702* from Eppendorf for one minute at 400 rpm instead of filtered, then acidified.

At NMBU was Agilent Technologies' *8800 ICP-MS Triple Quadrupole* together with Agilent Technologies' *SPS 4 Autosampler* used to analyse samples for metals.

2.3 Experimental setup

Firstly, three different experiments were performed in the lab at NMBU with model water based on the results from the analysis of the AMD collected 07.02.2022. Lastly, precipitation experiments and adsorption batch tests were performed at NMBU with preserved AMD collected 02.05.2022.

Chitosan and biochar Kitoflokk^{TM} 200 was obtained from Teta vannrensing AS. The chitosan solution was mixed 50/50 with DI water to get Kitoflokk^{TM} 100, used in the experiments. For biochar was biochar made of pig manure as feedstock used. More details can be found in Cuprys et al., 2021.

Model water

To make model water, the metal composition of the AMD was analysed. The samples were prepared, first filtered, and then acidified with nitric acid and with sulphuric acid.

Based on the results from the first ICP-MS run, two different types of model water were made. One of the types was made with the most significant (in quantity) metals in the AMD, which where Al, Ca, Cu, Fe, Mg, Mn, and Zn. The metal salts used was aluminium sulphate octadecahydrate, calcium sulphate dihydrate, iron(II) sulphate heptahydrate, copper(II) sulphate pentahydrate, zinc sulphate heptahydrate, magnesium sulphate heptahydrate, and manganese(II) chloride tetrahydrate.

Chitosan-covered biochar

Firstly was 30 mL of Kitoflokk^{TM} 200 and 30 mL of acetic acid 2% mixed together with 1 g of biochar. The solution was stirred for a little over four hours at 150 rpm. The mixture was added dropwise with a pipette into 2.5% NaOH and left in room temperature overnight. The NaOH was washed off the next day and dried in the oven at 105°C.

2.3.1 Adsorption batch experiments

The goal of the adsorption batch experiments is to see the removal efficiency of the adsorption materials in acidic pH levels. The adsorption materials of interests are biochar and chitosan-covered biochar beads, as used by Cuprys et al., 2021. For each of the materials, one experiment with different pH levels and a second experiment with different dosage in the same pH level, was conducted. In addition, was two last adsorption tests with the most optimal dose of beads and biochar performed with the preserved AMD from Folldal. In total six adsorption batch experiments were performed.

Experimental set-up

The adsorption material was weighted in polypropylene containers. After getting the wanted weight of adsorption material in all containers, 20 mL of model water or AMD was added. The containers were then put to mix overnight (12 hours for the preliminary tests with model water, 24 hours for the tests with AMD), and next day the volume needed for measuring metal residue was extracted with a 10-mL volume pipette. The rest of the water and the adsorption material was then properly disposed of.

Optimal dosage For finding the optimal dose of adsorption material, five different doses were tested in 20 mL of model water in pH 3.6. Two replicas of each dose together

with one matrix blank (the model water/AMD without the added materials) were continuously mixed at 150 rpm with *PSU-20i Multi-functional Orbital Shaker* from BioSan overnight. The different doses are:

- 1.00 g/L,
- 2.50 g/L,
- 5.00 g/L,
- 7.50 g/L,
- 10.0 g/L.

Optimal pH To find the most optimal pH for the adsorption material, a range of acidic pH was tested with a fixed dose of 2.5 g/L with the adsorption material. The lower dosage was chosen so the influence of pH could be seen in the results. Matrix blank and two replicas of each pH were continuously mixed at 150 rpm with a magnetic stirrer overnight. The different pH's are:

- pH 2.6,
- pH 3,
- pH 4.

Optimal dose with AMD The last batch adsorption tests were performed with three replicas of the most optimal dose of chitosan-covered biochar and of biochar, found in the experiments with the model water. The experiment was done with 20 mL of preserved AMD, added with 0.410 mL of 10M NaOH to adjust the pH value to ∼2.6, around the average pH found in the AMD from Folldal. Together in the run with each adsorption material was three matrix blanks adjusted to pH 2.6 and two more blanks.

2.3.2 Jar tests with chitosan as primary coagulant

The goal of the jar tests performed with chitosan as a primary coagulant at low pH is to get an indication of the efficiency of chitosan in very acidic waters (like AMD). Although the use of chitosan as a flocculant aid have been discussed and been in focus, there have been other experiments with the use of polymers as primary coagulants (Bratby, 2016; Renault et al., 2009). The objective of the jar tests now is therefore to get an indication of removal efficiency using Kitoflokk^{TM} 100 in acidic waters. The jar test equipment used was *Flocculator 2000* from Kemira with 1 L glass beakers. Different dosage and different pH values were tested, including matrix blanks for each pH value.

Experimental set-up

500 mL of model water was added to the beaker. The dose was added, and the program started immediately after. Based on recommendation from the producer of Kitoflokk^{TM} 100, and on literature, the program was set to:

- 60 seconds with 400 rpm,
- 15 minutes with 40 rpm,
- 30 minutes with settling.

Optimal pH To find the most optimal acidic pH to use Kitoflokk^{TM} 100, a fixed dose of 0.20 mL/L was used on different acidic pH's. The experiments were performed with one of each following pH values, including a matrix blank from each:

- pH 2.6,
- pH 3,
- pH 4.

Optimal dosage To find the optimal dosage of Kitoflokk^{TM} 100 in acidic water, three different doses and a matrix blank was tested in model water with pH 3.6. Based on recommendation from the producer, the chosen doses were:

- 0.15 mL/L,
- 0.20 mL/L,
- 0.25 mL/L.

2.3.3 Jar tests with chitosan as flocculant aid

The goal of the jar tests experiments with chitosan as flocculant aid to NaOH is to find out if chitosan is able to enhance the removal of metals during hydroxide precipitation. Two experiments were conducted, one with copper only model water (at MSU) and one with AMD (at NMBU). Five different doses of Kitoflokk^{TM} 100 were assessed. Together with matrix blank, three replicas of each dose were performed. All jars had the pH first raised to nine with NaOH. Due to the results from the first precipitation experiments performed at MSU being delayed, the objective of using chitosan as flocculation aid changed to see if it affects the process in a pH where most of the copper will be precipitated anyways.

After deciding on which pH value to continue the experiments with, experiments with Kitoflokk^{TM} 100 as flocculant aid was performed. The dosage of Kitoflokk^{TM} 100 added are:

- 0.35 mL/L,
- 0.40 mL/L,
- 0.45 mL/L,
- 0.50 mL/L,
- 0.55 mL/L.

0.950 L of AMD was used in each jar. The pH was first raised to pH 9 with NaOH. The flocculation program initiated was

- 60 seconds with 300 rpm,
- 10 minutes with 80 rpm,
- 1 hour with settling.

Kitoflokk^{TM} 100 was added after 30 seconds of rapid mixing. After settling was pH and conductivity measured, and samples extracted for metal analysis with ICP-MS.

3. Results and discussion

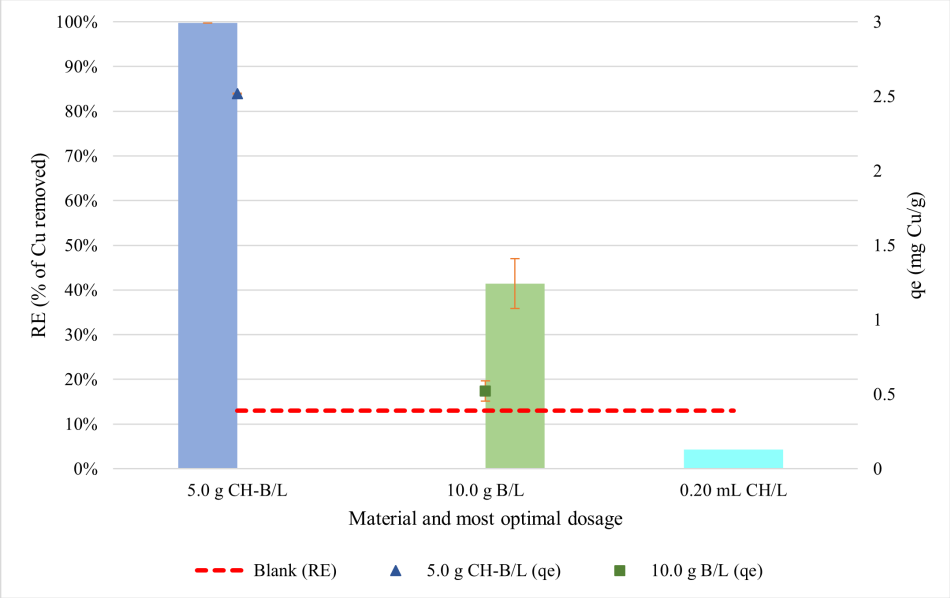

Figure 3.1: Comparing removal efficiency (**RE**, %) of Cu from model water in pH 3.6, between the most optimal dosage of chitosan-covered biochar (**CH-B**, 5.0 gram per litre of model water), biochar (**B**, 10.0 gram per litre of model water), and Kitoflokk^{TM} 100 (**CH**, 0.20 millilitres per litre of model water). Adsorption capacity (**qe**, milligram Cu per gram adsorption material) is included. *Blank* (red line) presents the removal of copper in model water at pH 3.6, without anything added.

The most optimal dosage (based on Cu removal) for each material from the first experiments performed at NMBU (adsorption batch test with CH-B and biochar, and Kitoflokk^{TM} 100 as primary coagulant) is illustrated in Figure 3.1. Chitosan as primary coagulant did not remove any Cu, while as CH-B

3.1 Metal concentration

Based on the results from the ICP-MS analysis of the first samples collected in Folldal, the chosen concentration of the model water is presented in Table 3.1. The metals chosen were the ones present in relatively large quantities. The results from the ICP-MS analysis is presented in Table F.1 in Appendix F on page 57. Based on earlier

Table 3.1: The concentration of metals (microgram per litre water) in the model water used for the first round of adsorption batch tests and for jar tests with Kitoflokk^{TM} 100 as primary flocculant.

Metal	Dosage (µg/L)
Aluminium	37504
Calcium	3406
Copper	12641
Iron	165179
Magnesium	50785
Manganese	13325
Zinc	8505

measurements (Table 1.1), this measurement is considerable lower than the average and most of the lowest measurements in the last five years. The weather for the seven days prior to the sampling shows some but little precipitation (Figure 2.3), however, the period had much higher precipitation than normal for the period, as mentioned earlier (2.1.1 on page 22). The temperature for the same period was warmer than the normal, but still below zero for most of the days.

The results from samples collected 02.05.22 is presented in Table F.3. The levels are higher than the results from the first samples, however, still lower concentration than the average concentration of metals (Table 1.1). The weather for the seven prior days (Figure 2.4) shows almost zero precipitation and positive mean temperatures. The period was much drier than the normal, as mentioned earlier (2.1.1 on page 22). Although the dry weather means less precipitation to dilute the stream, this is only a considerable effect seen during the spring flood and not when it precipitates for example during autumn. The samples were taken just after/around the period for the spring flood. Even if the period was dry, the melting of snow will contribute to the dilution of the stream. The concentration of metals are around the same as seen for the previous years in the same time (Table 1.3).

3.2 Adsorption batch tests

The results from the first adsorption batch test (with model water) is presented in Table F.2. The removal efficiency and adsorption capacity for biochar and chitosan-covered biochar under the different dosage and pH is presented for each metal in Figure E.2 and Figure E.3 in Appendix E on page 53. In summary, the removal efficiency of the

different doses of chitosan-covered biochar and biochar is illustrated in Figure 3.2 and Figure 3.3, together with the removal efficiency from a matrix blank with no adsorption materials. The corresponding adsorption capacity for each adsorption material is illustrated together in Figure 3.4.

Simultaneously is the removal efficiency of a fixed dose of CH-B and biochar in different acidic pH values presented in Figure 3.5 and Figure 3.6, together with the matrix blanks for each pH. The corresponding adsorption capacity for each adsorption material is illustrated together in Figure 3.7.

The mentioned figures show that CH-B is able to remove more of all metals measured than biochar alone at the same dose and also have a higher adsorption capacity than biochar alone. While biochar was able to remove nearly 100% of Al at the highest dose tested (10.0 g/L), the removal of all the other metals measured is never on the same level as for the removal efficiency with CH-B.

The removal efficiency of the most optimal dosages of CH-B and biochar in raw AMD, is presented in Table F.4 and illustrated in Figure 3.8 for all metals analysed for. The removal efficiency and the adsorption capacity of the metals with a positive removal rate is presented in Figure 3.9.

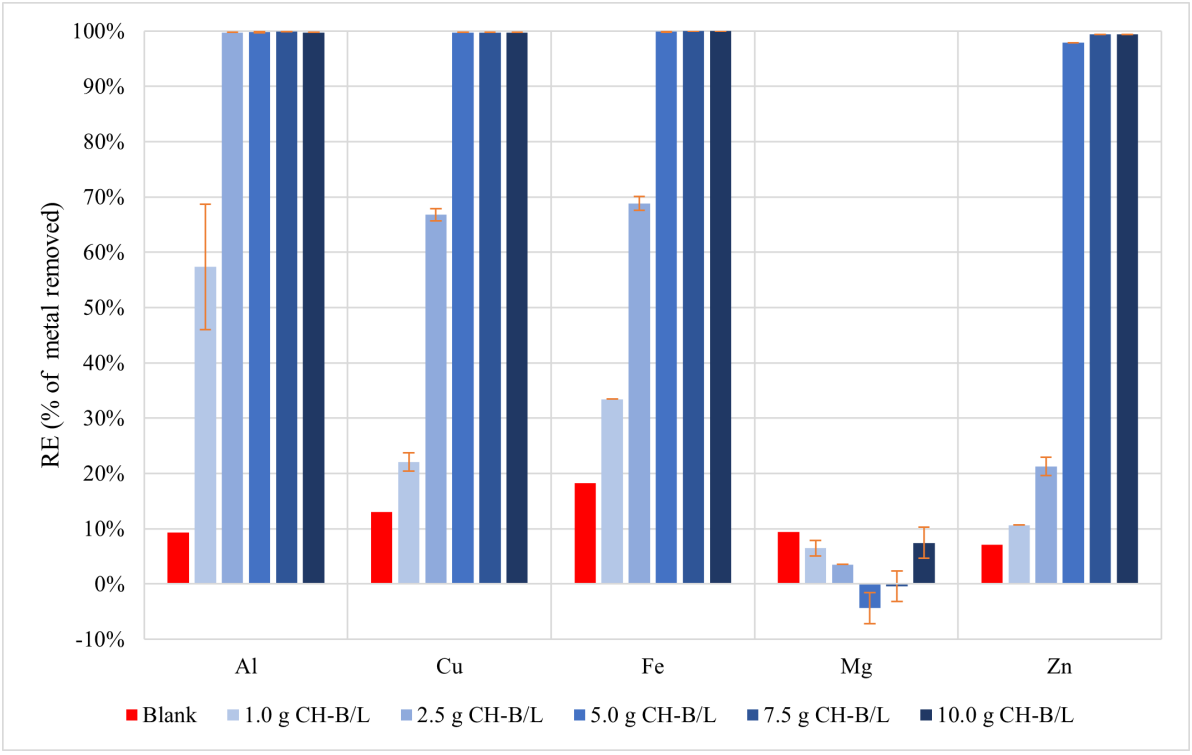

Figure 3.2: Diagram presenting the removal efficiency (**RE, %**) with different doses of chitosan-covered beads (**CH-B**, gram per litre of model water) in model water with pH 3.6. *Blank* is model water at the same pH value but without any adsorption material.

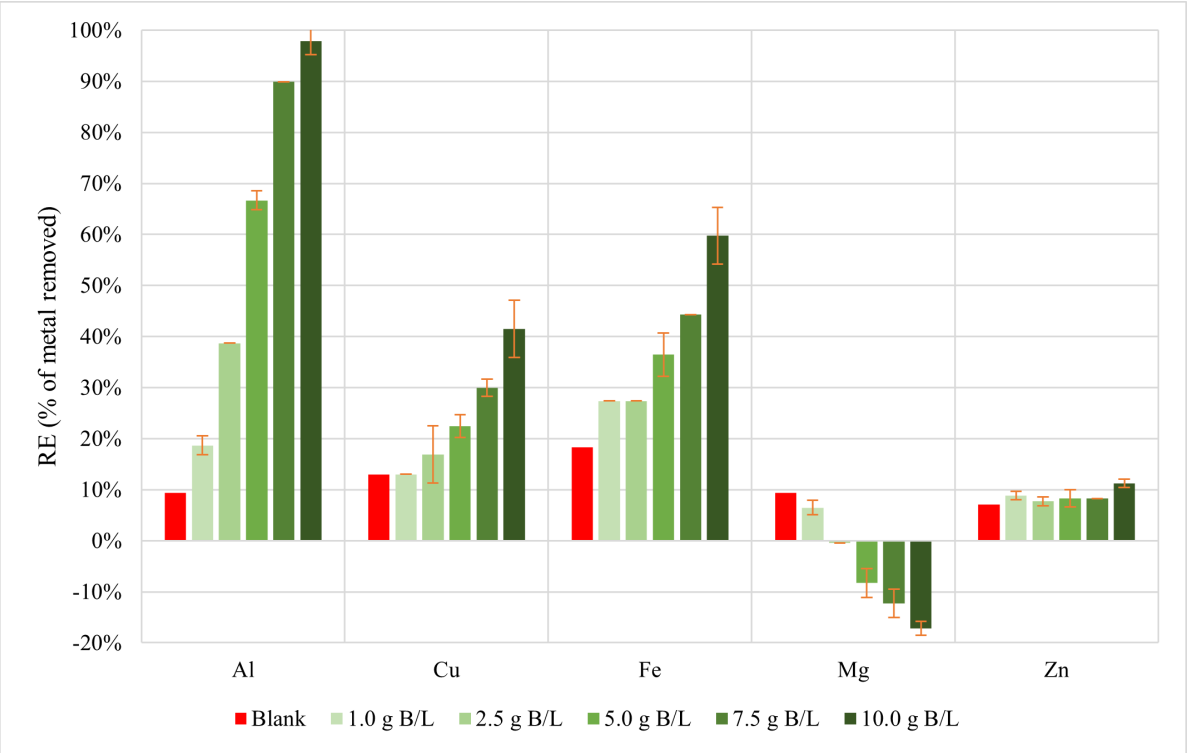

Figure 3.3: Diagram presenting the removal efficiency (**RE, %**) with different doses of biochar (**B**, gram per litre of model water) in model water with pH 3.6. *Blank* is model water at the same pH value but without any adsorption material..

The results for the adsorption batch tests with collected AMD does not follow the results seen in the experiments with model water. Now only Fe and Cr are removed, while Al is leaking from the CH-B, opposite from the nearly 100% removal from model water. Additionally to Al is also Mg, Ca and Mn leaking in considerable numbers from the CH-B and also the biochar. No removal of Cd, Zn, or Cu is observed either.

The results are also differing from other experiments performed with modified chitosan on raw waters (Laus et al., 2007; Song et al., 2021). This gives an indication that there are other important parameters in the water matrix of the AMD that needs to be investigated. No tests were done for sulphate or other sulfuric elements, although the annual reports made for DMF shows high concentration of sulphate.

Overall, modifying the biochar with chitosan to CH-B improves the removal efficiency and adsorption capacity both for model water and AMD. Additionally is CH-B leaking less metals than the biochar alone (beside for the Al in AMD). The addition of chitosan, which has more functional groups, results in higher removal than with biochar alone.

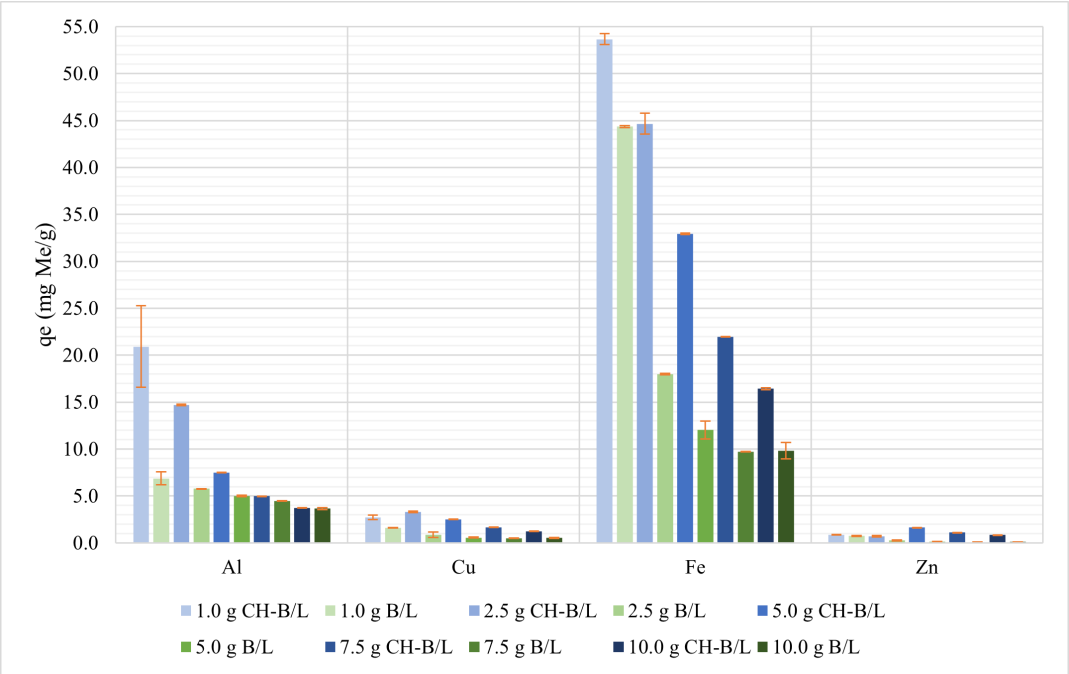

Figure 3.4: Diagram presenting adsorption capacity (**qe**) for different doses of chitosan-covered biochar (**CH-B**, in blue) and biochar (**B**, in green) in model water with pH 3.6. The qe is given in milligram of metal (**Me**) per gram of adsorption material, and doses of adsorption material in gram per litre model water.

3.3 Chitosan as primary coagulant

The results from the experiments with Kitoflokk^{TM} 100 as primary coagulant is illustrated in Figure E.1. Performance of both different doses (0.15 mL/L, 0.20 mL/L, 0.25 mL/L) in pH level 3.6, and the performance of 0.20 mL of Kitoflokk^{TM} 100 per litre in different acidic pH levels (2.6, 3.0, 3.6, 4.0) is shown. The results indicates there have not been any removal of any metals with the use of Kitoflokk^{TM} 100 as primary coagulant in acidic levels. Contrary, when it comes to Al, it seems like Kitoflokk^{TM} 100 somehow reduces the removal of Al compared to the matrix blank. This goes for both different doses and different pH values.

3.4 Chitosan as flocculant aid

Due to late results from the experiments with different pH, the objective of the experiment was change to see if chitosan as flocculant aid would affect the precipitation of metals with NaOH. pH 9 was chosen to be sure most metals precipitates. The results from the experiments with Kitoflokk^{TM} 100 as flocculant aid in raw water/AMD is presented in Table F.5. The change in pH after sedimentation for each of the dosages of Kitoflokk^{TM} 100 and matrix blank is illustrated in Figure 3.10. The results shows nearly 100% removal of all metal analysed beside Mg and Ca. This includes for all the doses of

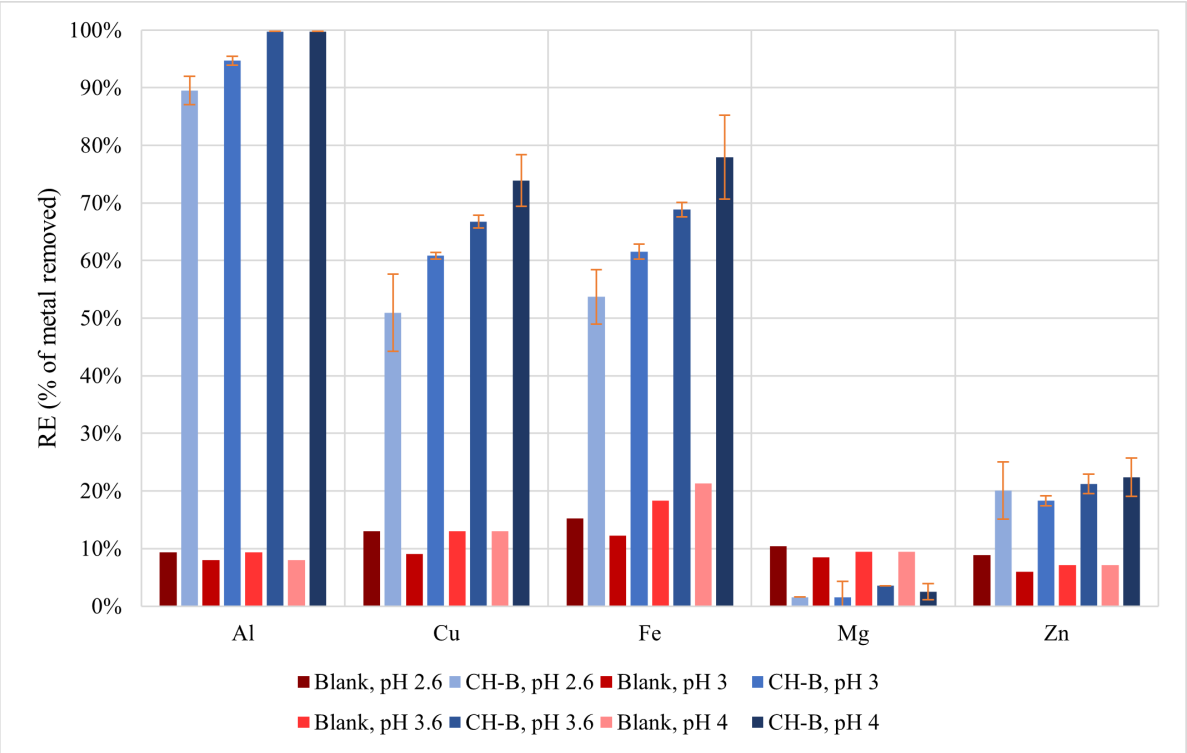

Figure 3.5: Diagram presenting the removal efficiency (**RE, %**) with a fixed-dose of chitosan-covered biochar (**CH-B**, 2.5 gram per litre of model water) in model water with different pH values. *The blanks* are model water at the same pH values but without any adsorption material.

Kitoflokk^{TM} 100 as flocculant aid and the matrix blank with only NaOH added. While Kitoflokk^{TM} 100 did not affect the removal, it did however affect the final pH. Figure 3.10 show that the final pH, after one hour of settling, is sinking with the increasing dose of Kitoflokk^{TM} 100. Additionally, it was observed that the sludge was changing, seen in Figure D.1. The sludge was not further analysed, but the volume has increased with the addition of Kitoflokk^{TM} 100.

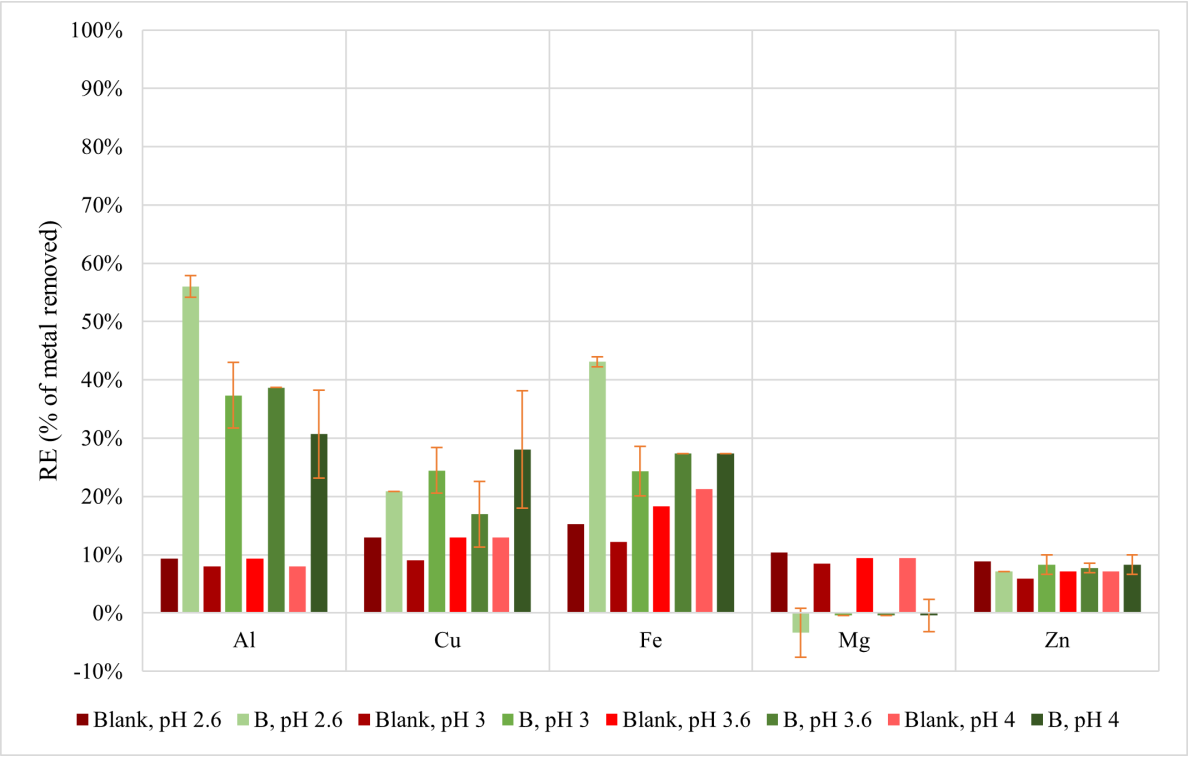

Figure 3.6: Diagram presenting the removal efficiency (**RE, %**) with a fixed-dose of biochar (**B**, 2.5 gram per litre of model water) in model water with different pH values. *The blanks* are model water at the same pH values but without any adsorption material.

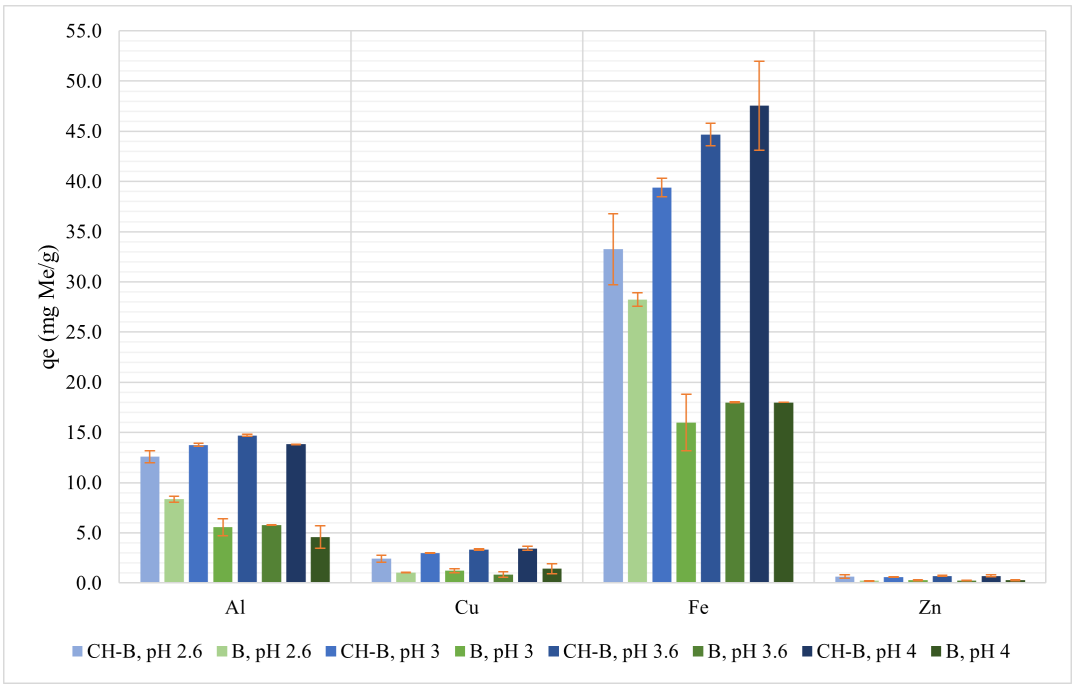

Figure 3.7: Diagram presenting adsorption capacity (**qe**) for a fixed-dose (2.5 gram per litre model water) of chitosan-covered biochar (**CH-B**, in blue) and biochar (**B**, in green) in model waters with different pH values. The qe is given in milligram of metal (**Me**) per gram of adsorption material.

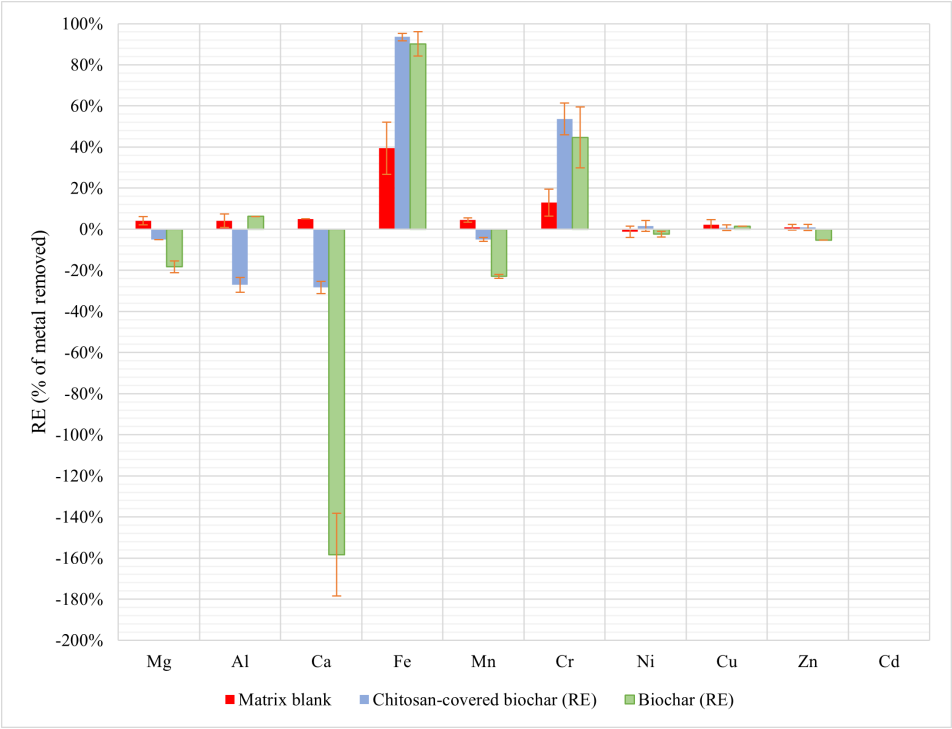

Figure 3.8: Diagram presenting removal efficiency (**RE**, %) from adsorption batch tests with 5.0 gram of chitosan-covered biochar (**CH-B**, blue) per litre AMD and with 10.0 gram of biochar (**B**, green) per litre AMD. Matrix blank (red) is AMD without any adsorption material but with the same pH value (2.6).

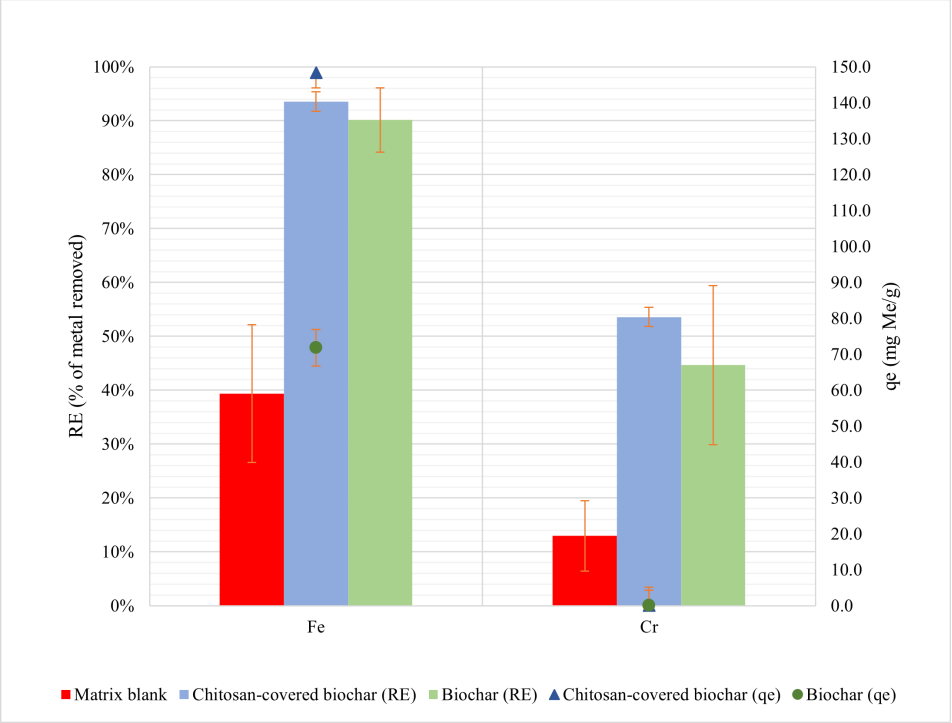

Figure 3.9: Diagram presenting removal efficiency (**RE**, %) and adsorption capacity (**qe**, milligram of metal (**Me**) per gram adsorption material) from adsorption batch tests. Removed Fe and Cr with 5.0 grams of chitosan-covered biochar (**CH-B**, blue) per litre AMD and with 10.0 grams of biochar (**B**, green) per litre AMD. Matrix blank (red) is AMD without any adsorption material but with the same pH value (2.6).

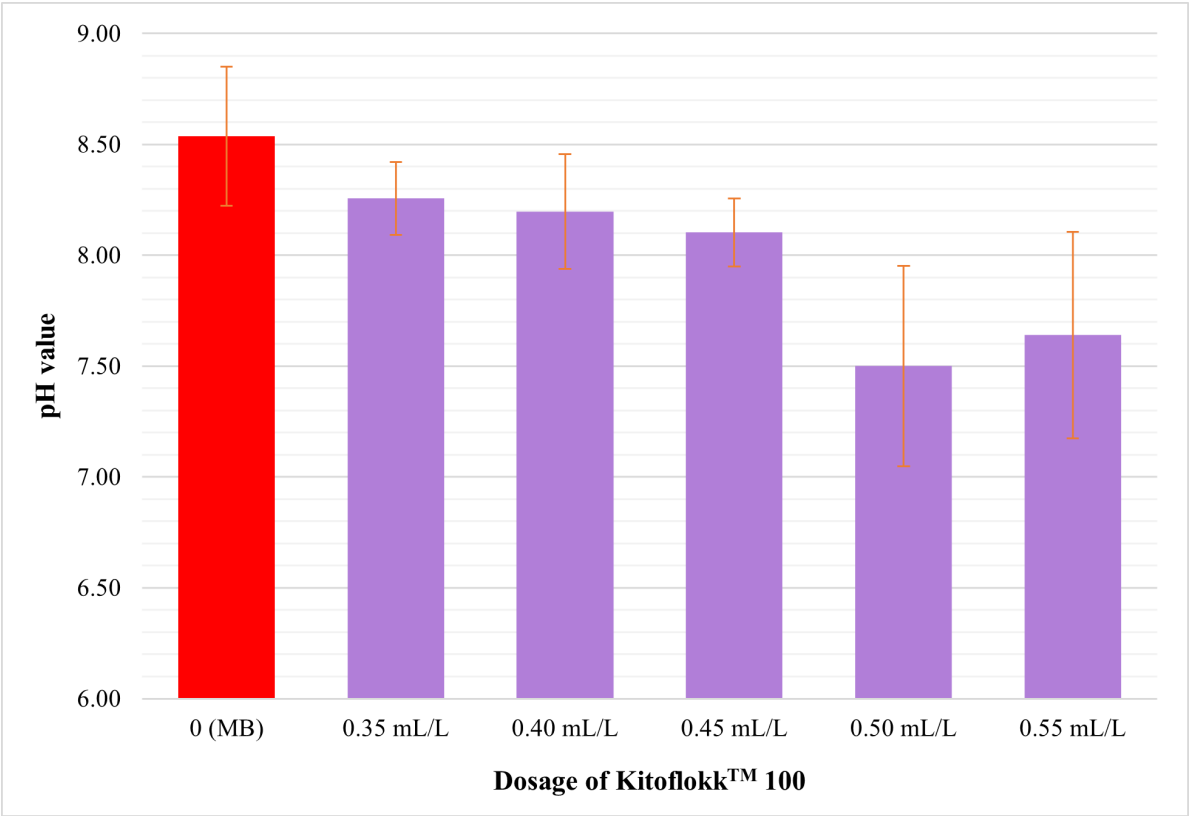

Figure 3.10: Diagram illustrating the pH of the supernatant in the jar tests with Kitoflokk^{TM} 100 (purple) as flocculant aid after one hour with settling. Kitoflokk^{TM} 100 given in millilitre per litre AMD. Matrix blank (**MB**, red) is AMD raised to pH 9 with NaOH but without any Kitoflokk^{TM} 100 as flocculant aid.

4. Conclusions

Different novel methods have been covered by several experiments on different technologies with nature-derived chemicals.

There are no promising results with using chitosan as a primary coagulant in acidic water. The chitosan as flocculant aid does not influence the removal rate with NaOH. However, an increase in sludge volume is not ideal. Research is needed into the sludge composition and if this is also observed in lower pH ranges.

The experiments with model water show promising results in using chitosan-covered biochar to remove metals from acidic waters. Still, the results from the same experiments but with AMD indicate other parameters in the water matrix of AMD involved in the removal process that needs to be investigated further. The results also show how unique each case can be, that the results from research on AMD from other mines not necessarily can be transferred to other cases, and that individual assessment for each case is needed.

The results in this thesis indicate that there are prospects for using nature-derived chemicals and novel methods when removing metals from AMD; however, more research is needed to draw any conclusions to the research questions introduced in Section 1.8 on page 17.

Adsorption in model water is comparable with NaOH use; still, more research is needed on adsorption in raw water. Coagulation with chitosan as the primary coagulant in acidic water is not removing any metal. The combination of adsorption with CH-B and conventional methods was not investigated, and experiments with chitosan as a flocculant aid is not providing enough data to compare its performance.

Future recommendations should research the role of different parameters in AMD and their interaction with nature-derived chemicals. The possibility of using nature-derived chemicals as an adsorbent in a secondary treatment after the use of conventional methods should be investigated, and so if it can reduce the cost of conventional chemicals and possibly sludge volume. The regeneration of chitosan-covered biochar and metal recovery is also of interest, as it might reduce the cost of chemicals needed.

Reference

Akcil, A. and Koldas, S. (Jan. 2006). *Acid Mine Drainage (AMD): causes, treatment and case studies*. DOI: 10.1016/j.jclepro.2004.09.006.

Amacher, M. C., Brown, R. W., Kotuby-Amacher, J., and Willis, A. (1993). *Adding Sodium Hydroxide To Study Metal Removal in a Stream Affected by Acid Mine Drainage*. Tech. rep. Ogden, UT: Intermountain Research St: 17. URL: https://books.google.no/books?id=Yja5Nm1iKC4C&dq=sodium%20hydroxide%20acid%20mine%20drainage&lr&hl=no&pg=PA1#v=onepage&q&f=false.

American Public Health Association, American Water Works Association, and Water Environment Federation (2012). *Standard Methods For the Examination of Water and Wastewater*. Ed. by E. W. (Rice, R. B. (Baird, A. D. (Eaton, and L. S. (Clesceri. 22nd ed. Washington, DC: American Public Health Association: 1496.

Balintova, M. and Petrilakova, A. (2011). Study of pH influence on selective precipitation of heavy metals from acid mine drainage. In: *Chemical Engineering Transactions*. Vol. 25: 345–350. DOI: 10.3303/CET1125058.

Bessho, M., Markovic, R., Trujic, T. A., Masuda, N., Bozic, D., and Stevanovic, Z. (2019). Recovery of Metals from Acid Mine Drainage Using Organic Polymer. In: *Mine Water: Technological and Ecological Challenges*. Ed. by C. Wolkersdorfer, E. Khayrulina, S. Polyakova, and A. Bogush. Perm: International Mine Water Association: 155–160. DOI: 10.3303/CET1228019.

Bratby, J. (2016). *Coagulation and Flocculation in Water and Wastewater Treatment*. 3rd ed. Vol. 15. London: IWA Publishing: 524. DOI: 10.2166/9781780407500.

Brião, G. d. V., de Andrade, J. R., da Silva, M. G. C., and Vieira, M. G. A. (July 2020). *Removal of toxic metals from water using chitosan-based magnetic adsorbents. A review*. DOI: 10.1007/s10311-020-01003-y.

Cuprys, A., Maletskyi, Z., Rouissi, T., Ratnaweera, H., Brar, S. K., Knystautas, E., and Drogui, P. (2021). Insights into the simultaneous sorption of ciprofloxacin and heavy metals using functionalized biochar. *Water* 13 (19): 20. DOI: 10.3390/w13192768.

Direktoratet for mineralforvaltning med Bergmesteren for Svalbard (Mar. 2015). *Miljøtiltak | Direktoratet for Mineralforvaltning*. URL: https://www.dirmin.no/tema/miljotiltak.

Direktoratet for mineralforvaltning ved Bergmesteren i Svalbard (2022). *Helhetlig tiltaksplan for Folldal gruver*. Tech. rep. Trondheim: Direktoratet for mineralforvaltning med Bergmesteren for Svalbard: 28. URL: https://www.dirmin.no/sites/default/files/folldal_gruve_-_oversendelse_av_helhetlig_tiltaksplan_og_anbefaling_og_helhetlig_tiltaksplan_1.pdf.

Evangelou, V. (1998). *Environmental Soil and Water Chemistry: Principles and Applications*. Lexington, Kentucky: John Wiley and Sons Inc.: 592.

Evensen, L. (2021). *Overvåkning av gruvepåvirkede vassdrag ved Folldal Verk - Årsrapport 2020*. Tech. rep. Trondheim: Norconsult AS: 0–42.

Evensen, L. and Simonsen, L. (2022). *Overvåkning av gruvepåvirkede vassdrag ved Folldal Verk - Årsrapport 2021*. Tech. rep. Norconsult AS: 47.

Folldal kommune (2021). *Handlingsplan gruveforurensning Folldal sentrum*. Folldal.

Gao, N., Du, W., Zhang, M., Ling, G., and Zhang, P. (June 2022). Chitosan-modified biochar: Preparation, modifications, mechanisms and applications. *International Journal of Biological Macromolecules* 209: 31–49. DOI: 10.1016/j.ijbiomac.2022.04.006.

Gidas, W.-B., Garnier, O., and Gidas, N. (1999). Performance of chitosan as a primary coagulant for the wastewater treatment. In: *Water Pollution V*. Ed. by C. Brebbia and P. Anagnostopoulos. Vol. 33. WIT Press: 47–56. DOI: 10.2495/WP990051.

Grinde, L., Mamen, J., and Tunheim, K. (2022a). *Været i Norge - Klimatologisk månedsoversikt februar 2022 og vintersesongen 2021/2022*. Tech. rep. Oslo: Meteorologisk institutt: 36. URL: https://www.met.no/publikasjoner/met-info.

Grinde, L., Mamen, J., and Tunheim, K. (2022b). *Været i Norge - Klimatologisk månedsoversikt januar 2022*. Tech. rep. Oslo: Meteorologisk institutt: 23. URL: https://www.met.no/publikasjoner/met-info.

Grinde, L., Mamen, J., and Tunheim, K. (2022c). *Været i Norge: Klimatologisk månedsoversikt april 2022*. Tech. rep. Oslo: Meteorologisk institutt: 21. URL: https://www.met.no/publikasjoner/met-info.

Gvein, Ø., Rui, I. J., and Dahl, R. M. (n.d.). *Bergverksdrift i Norge – Store norske leksikon*. URL: https://snl.no/Bergverksdrift_i_Norge.

Igberase, E., Osifo, P., and Ofomaja, A. (2018). Mathematical modelling of Pb2+, Cu2+, Ni2+, Zn2+, Cr6+ and Cd2+ ions adsorption from a synthetic acid mine drainage onto chitosan derivative in a packed bed column. *Environmental Technology (United Kingdom)* 39 (24): 3203–3220. DOI: 10.1080/09593330.2017.1375027.

Iversen, E. R. (2000). *Oppfølging av forurensningstilførsler fra Folldal sentrum. Undersøkelser i 1999*. Tech. rep. Hedmark: Norsk institutt for vannforskning: 26. URL: http://hdl.handle.net/11250/210954.

Iversen, E. R. and Arnesen, R. T. (2003). *Elvestrekninger påvirket av gruveforurensning*. Tech. rep. Oslo: Norsk Institutt for Vannforskning, NIVA: 81. URL: https://www.miljodirektoratet.no/globalassets/publikasjoner/klif2/publikasjoner/kjemikalier/1986/ta1986.pdf.

Johnson, D. B. (2003). Chemical and microbiological characteristics of mineral spoils and drainage waters at abandoned coal and metal mines. *Water, Air, and Soil Pollution: Focus* 3 (1): 47–66. DOI: 10.1023/A:1022107520836.

Johnson, D. B. and Hallberg, K. B. (Feb. 2005). Acid mine drainage remediation options: A review. *Science of the Total Environment* 338 (1-2 SPEC. ISS.): 3–14. DOI: 10.1016/j.scitotenv.2004.09.002.

Kefeni, K. K., Msagati, T. A., and Mamba, B. B. (May 2017). *Acid mine drainage: Prevention, treatment options, and resource recovery: A review*. DOI: 10.1016/j.jclepro.2017.03.082.

Kim, N. and Park, D. (Sept. 2021). *Biosorptive treatment of acid mine drainage: a review*. DOI: 10.1007/s13762-021-03631-5.

Knutzen, J., Green, N., and Lingsten, L. (1986). *Forekomst av miljøgifter i norske vassdrag og fjorder. Rapport 1: Hovedrapport*. Tech. rep. Norway: Norsk institutt for vannforskning: 95. URL: http://hdl.handle.net/11250/204700.

Laus, R., Geremias, R., Vasconcelos, H. L., Laranjeira, M. C., and Fávere, V. T. (Oct. 2007). Reduction of acidity and removal of metal ions from coal mining effluents using chitosan microspheres. *Journal of Hazardous Materials* 149 (2): 471–474. DOI: 10.1016/j.jhazmat.2007.04.012.

Lewis, A. (2017). Precipitation of heavy metals. In: *Sustainable Heavy Metal Remediation. Environmental Chemistry for a Sustainable World*. Ed. by E. Rene, E. Sahinkaya, A. Lewis, and P. N. L. Lens. Vol. 8. Springer, Cham. Chap. Chapter 4: 101–120. DOI: 10.1007/978-3-319-58622-9{_}4.

Løkken, T. H. (Apr. 2022a). *Frustrasjon over brev : - Hårreisende*. URL: https://www.ostlendingen.no/frustrasjon-over-brev-harreisende/s/5-69-1292687?key=2022-05-01T10:46:33.000Z/retriever/22297c6ff5ff1f728a381f54e8a7bc613bce5ba3.

Løkken, T. H. (Mar. 2022b). *Grøftesystem og survannsnett kan utbedres allerede i 2022*. URL: https://www.retten.no/groftesystem-og-survannsnett-kan-utbedres-allerede-i-2022/s/5-44-619947?key=2022-04-28T13:36:37.000Z/retriever/1c92aca60848f829f4116ac4114f9a

Løvdal, Ø. (2016). *Overvåking av gruvepåvirkede vassdrag ved Folldal gruver - Årsrapport 2015*. Tech. rep. Oslo: COWI AS: 1–17.

Manstad-Hulaas, A. J. (2018). *Overvåking av gruvepåvirkede vassdrag ved Folldal gruver - Årsrapport 2017*. Tech. rep. Fredrikstad: COWI AS: 1–24.

Markovic, R., Bessho, M., Masuda, N., Stevanovic, Z., Bozic, D., Trujic, T. A., and Gardic, V. (2020). New approach of metals removal from acid mine drainage. *Applied Sciences (Switzerland)* 10 (17). DOI: 10.3390/app10175925.

Miljødirektoratet (2016). *Grenseverdier for klassifisering av vann, sediment og biota – revidert 30.10.2020*. Trondheim. URL: https://www.miljodirektoratet.no/globalassets/publikasjoner/M608/M608.pdf.

Muxika, A., Etxabide, A., Uranga, J., Guerrero, P., and de la Caba, K. (Dec. 2017). *Chitosan as a bioactive polymer: Processing, properties and applications*. DOI: 10.1016/j.ijbiomac.2017.07.087.

Norges geologiske undersøkelse (Dec. 2014). *Metaller | Norges geologiske undersøkelse*. URL: https://www.ngu.no/emne/metaller.

Okkenhaug, G., Breedveld, G., Kvennås, M., and Lundgren, T. (2015). *Folldal gruver - Vurdering av mulige tiltak mot avrenning fra tidligere gruvevirksomhet*. Tech. rep. Trondheim: Norges geotekniske institutt: 46. URL: https://www.dirmin.no/sites/default/files/folldal_-_tiltaksvurderinger.pdf%0A.

Pabst, T. and Kvennås, M. (2014). *Folldal Gruver. Kartlegging av avgangsmasser og vann*. Tech. rep. Folldal: Norges geotekniske institutt: 31.

Pivokonský, M., Novotná, K., Čermáková, L., and Petříček, R. (2022). *Jar Tests for Water Treatment Optimisation How to Perform Jar Tests*. IWA Publishing: 73. DOI: https://doi.org/10.2166/9781789062694.

Renault, F., Sancey, B., Badot, P. M., and Crini, G. (2009). *Chitosan for coagulation/flocculation processes - An eco-friendly approach*. DOI: 10.1016/j.eurpolymj.2008.12.027.

Rhazi, M., Tolaimate, A., Rhazi, M., Desbriéres, J., Tolaimate, A., Rinaudo, M., Alagui, A., and Vottero, P. (Feb. 2001). Contribution to the study of the complexation of copper by chitosan and oligomers. *Polymer* 43 (4): 1267–1276. DOI: 10.1016/S0032-3861(01)00685-1.

Rinaudo, M. (July 2006). Chitin and chitosan: Properties and applications. *Progress in Polymer Science (Oxford)* 31 (7): 603–632. DOI: 10.1016/j.progpolymsci.2006.06.001.

Sæland, F., Nyland, A. J., Østensen, P. Ø., Nordrum, F. S., and Kullerud, K. (2016). *Bergverk i Norge - kulturminner og historie*. Ed. by B. I. Berg. Kongsberg, Norge: Fagbokforlaget: 430.

Simate, G. S. and Ndlovu, S. (Sept. 2014). *Acid mine drainage: Challenges and opportunities*. DOI: 10.1016/j.jece.2014.07.021.

Song, J., Messele, S. A., Meng, L., Huang, Z., and Gamal El-Din, M. (Apr. 2021). Adsorption of metals from oil sands process water (OSPW) under natural pH by sludge-based Biochar/Chitosan composite. *Water Research* 194: 116930. DOI: 10.1016/j.watres.2021.116930.

Statens forurensningstilsyn (1992). *Deponier med spesialavfall, forurenset grunn og forurensede sedimenter: handlingsplan for opprydning*. Tech. rep. Grimstad: Statens Forurensningstilsyn: 74 s. URL: https://urn.nb.no/URN:NBN:no-nb_digibok_2009083101079.

Stiftelsen Folldal Gruver (n.d.). *Historie | Stiftelsen Folldal Gruver*. URL: https://folldalgruver.no/historien.

Stumm, W. and Morgan, J. J. (1995). *Aquatic Chemistry. Chemical Equilibria and Rates in Natural Waters*. Ed. by J. J. Schnoor and A. Zehnder. 3rd ed. Zurich, Pasadena: John Wiley & Sons, Ltd: 1040.

Sun, Y., Shah, K. J., Sun, W., and Zheng, H. (May 2019). Performance evaluation of chitosan-based flocculants with good pH resistance and high heavy metals removal capacity. *Separation and Purification Technology* 215: 208–216. DOI: 10.1016/j.seppur.2019.01.017.

Tuttle, K. and Simonsen, L. (2019). *Overvåkning av gruvepåvirkede vassdrag ved Folldal Verk - Årsrapport 2018*. Tech. rep. Norconsult AS: 51.

Tuttle, K. and Simonsen, L. (2020). *Overvåkning av gruvepåvirkede vassdrag ved Folldal Verk - Årsrapport 2019*. Tech. rep. Norconsult AS: 40.

Wang, J. and Wang, S. (Aug. 2019). Preparation, modification and environmental application of biochar: A review. *Journal of Cleaner Production* 227: 1002–1022. DOI: 10.1016/J.JCLEPRO.2019.04.282.

Yang, R., Li, H., Huang, M., Yang, H., and Li, A. (2016). *A review on chitosan-based flocculants and their applications in water treatment*. DOI: 10.1016/j.watres.2016.02.068.

Zhou, Y., Gao, B., Zimmerman, A. R., Fang, J., Sun, Y., and Cao, X. (Sept. 2013). Sorption of heavy metals on chitosan-modified biochars and its biological effects. *Chemical Engineering Journal* 231: 512–518. DOI: 10.1016/j.cej.2013.07.036.

Appendix A. Quality Standards Fresh Water

Table A.1: Values and limits for all monitored metals in fresh water and their classifications in Miljødirektoratet, 2016.

Element	Class I	Class II	Class III	Class IV	Class V
	Background	**Good**	**Moderate**	**Bad**	**Very bad**
As	0 - 0.15	0.15 - 0.5	0.5 - 8.5	8.5 - 85	>85
Pb	0 - 0.02	0.02 - 1.2	1.2 - 14	14 - 57	>57
Cd - $CaCO_3$ <40 mg/L - $CaCO_3$ 40 - <50 mg/L - $CaCO_3$ 50 - <100 mg/L - $CaCO_3$ 100 - <200 mg/L - $CaCO_3 \geq 200 mg/L$	0 - 0.003	≤ 0.08 0.08 0.09 0.15 0.25	≤ 0.45 0.45 0.6 0.9 1.5	≤ 4.5 4.5 6.0 9.0 15.0	>15.0
Cu	0 - 0.3	0.3 - 7.8		7.8 - 15.6	>15.6
Cr	0 - 0.1	0.1 - 3.4			>3.4
Hg	0 - 0.001	0.001 - 0.047	0.047 - 0.07	0.07 - 0.14	>0.14
Ni	0 - 0.5	0.5 - 4	4 - 34	34 - 67	>67
Zn	0 - 1.5	1.5 - 11		11 - 60	>60

Appendix B. Map of spoil masses

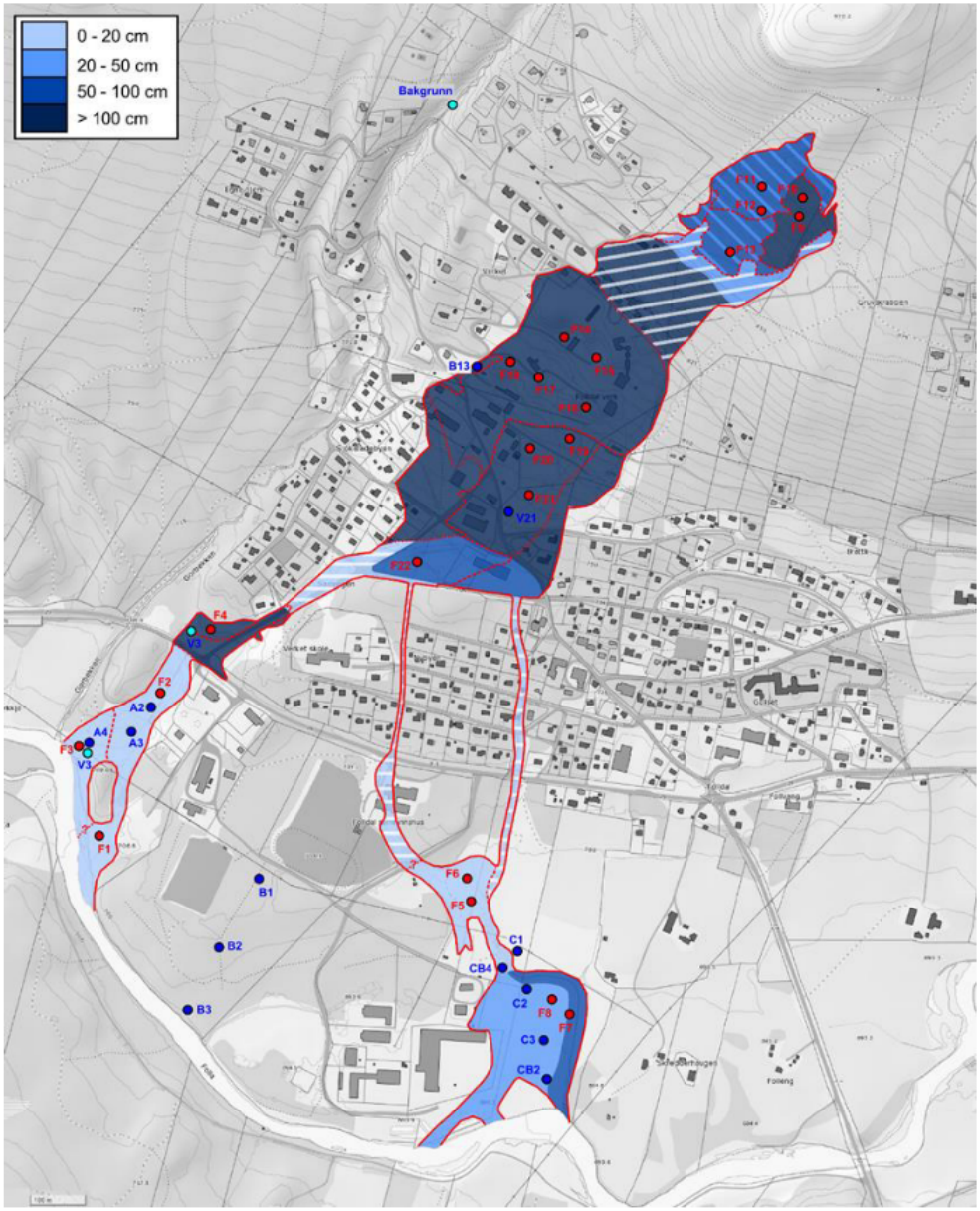

Figure B.1: Map of spoil masses in Folldal (Pabst and Kvennås, 2014). The blue colour indicate the depth of the spoil masses (the darker blue, the deeper). White stripes indicates low number of samples of the masses. Adapted with permission from DMF.

Appendix C. Material and methods - at MSU

Experiments were performed at MSU after the first experiments were performed at NMBU. Since the result were not ready in time for the finishing of this thesis, the method is described in this chapter in the appendix.

Equipments At MSU, the pH-meter used was *Fisher Scientific Accumet AB15*. *iCAPTM Q ICP-MS* from Thermo Scientific™ is used to analyse samples for metals together with CETAC Technologies' *Analyte G2 Excimer Laser Ablation System* with a 15 x 15 cm *HelEx*™ cell and *ASX-520 Autosampler*.

Model water The type of model water was made with copper only as it is the main target of removal. The intention with the two different model water is to compare the copper removal when there is copper only and then when other major metals is present. The experiments with copper only were performed with copper(II) sulphate from Sigma Aldrich as the metal salt.

Precipitation tests

The pH was adjusted with the use of NaOH, a hydroxide precipitation. Three different pH were used. Based on the chemistry of copper, pH 7, 8, and 9 was controlled. Three replicas of the experiment were performed, with a matrix blank each round. 1 L glass beakers were used for the experiments, together with magnetic stirrer.

One litre model water was added to the beaker. The model water was stirred slowly while pH was measured constantly. When the pH was stable, NaOH was added with a pipette. NaOH was added until reaching the desired pH (either 7, 8, or 9). The model water with precipitant was now mixed with magnetic stirrer. Based on other experiments, the mixing time is set to:

- 60 seconds with 300 rpm,
- 10 minutes with 80 rpm,
- 1 hour with settling.

After settling, the pH was again measured, and a picture was taken of the unit. The volume needed of the supernatant for measuring metal residue, was extracted by pipette. The rest of the supernatant and precipitate was appropriately disposed.

Jar tests with precipitation and chitosan as flocculant aid

The goal of the jar tests experiments with chitosan as flocculant aid to NaOH is to find out if chitosan is able to enhance the removal of metals during hydroxide precipitation. The jar tests at MSU were performed with the *PB-900TM Programmable JarTester*, which has six square plastic 2 L jars with a tap located 10 cm over the bottom. Five different doses of Kitoflokk^{TM} 100 were assessed. Together with matrix blank, three replicas of each dose were performed. With exemption of jars with matrix blanks, all jars had the pH first raised to nine with NaOH.

After deciding on which pH value to continue the experiments with, experiments with Kitoflokk^{TM} 100 as flocculant aid was performed. The dosage of Kitoflokk^{TM} 100 added are:

- 0.35 mL/L,
- 0.40 mL/L,
- 0.45 mL/L,
- 0.50 mL/L,
- 0.55 mL/L.

Two litre Cu-only model water was added to each jar. The paddles stirred the model water at 50 rpm so it properly mixed and the initial pH in each jar was first controlled. By adding NaOH with a pipette, the pH was increased to pH 9 in all jars while the paddles rotate at 50 rpm. When all units have pH raised to pH 9, the following program was initiated:

- 90 seconds with 300 rpm,
- 10 minutes with 80 rpm,
- 1 hour with settling.

The 30 extra seconds is for the flocculant aid to work, according to Bratby, 2016. The Kitoflokk^{TM} 100 was added between the 30th and 60th second of first round. The pH was measured in all jars after the settling period, and the volume of supernatant needed for measuring metal residue was extracted through the tap.

Appendix D. Pictures from jar test

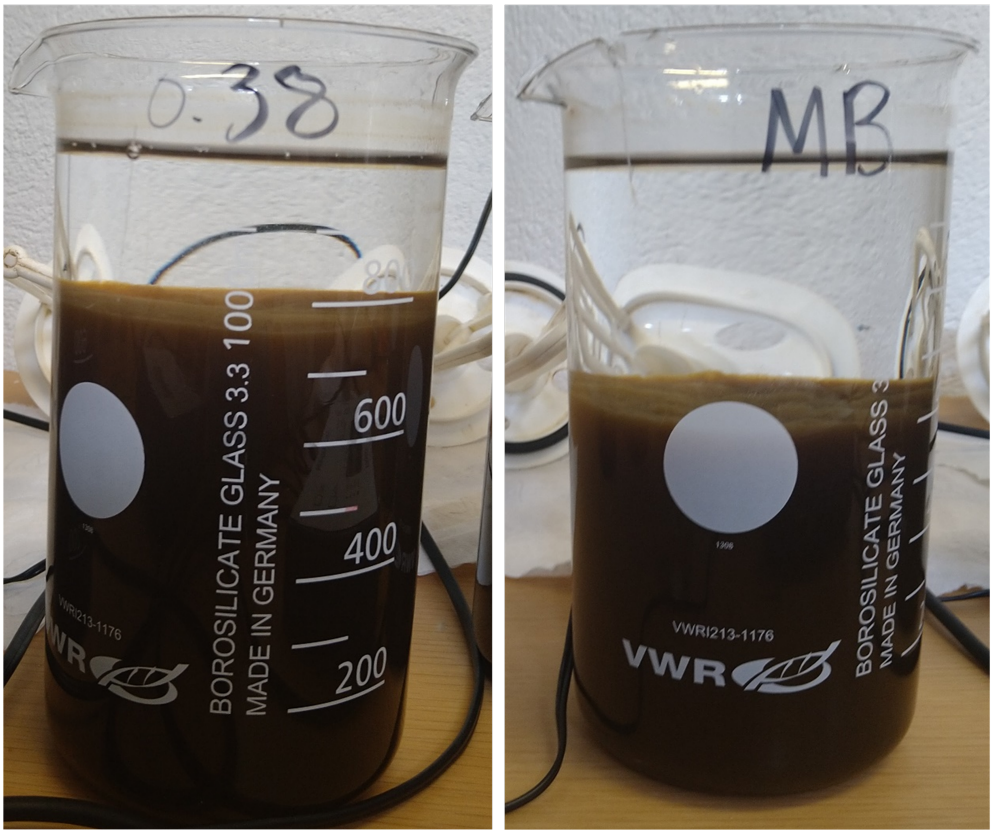

Figure D.1: Pictures of the jars after one hour with sedimentation. To the left is a jar added with a dose of KitoflokkTM 100, to right is a jar with only NaOH.

Appendix E. Results in diagrams

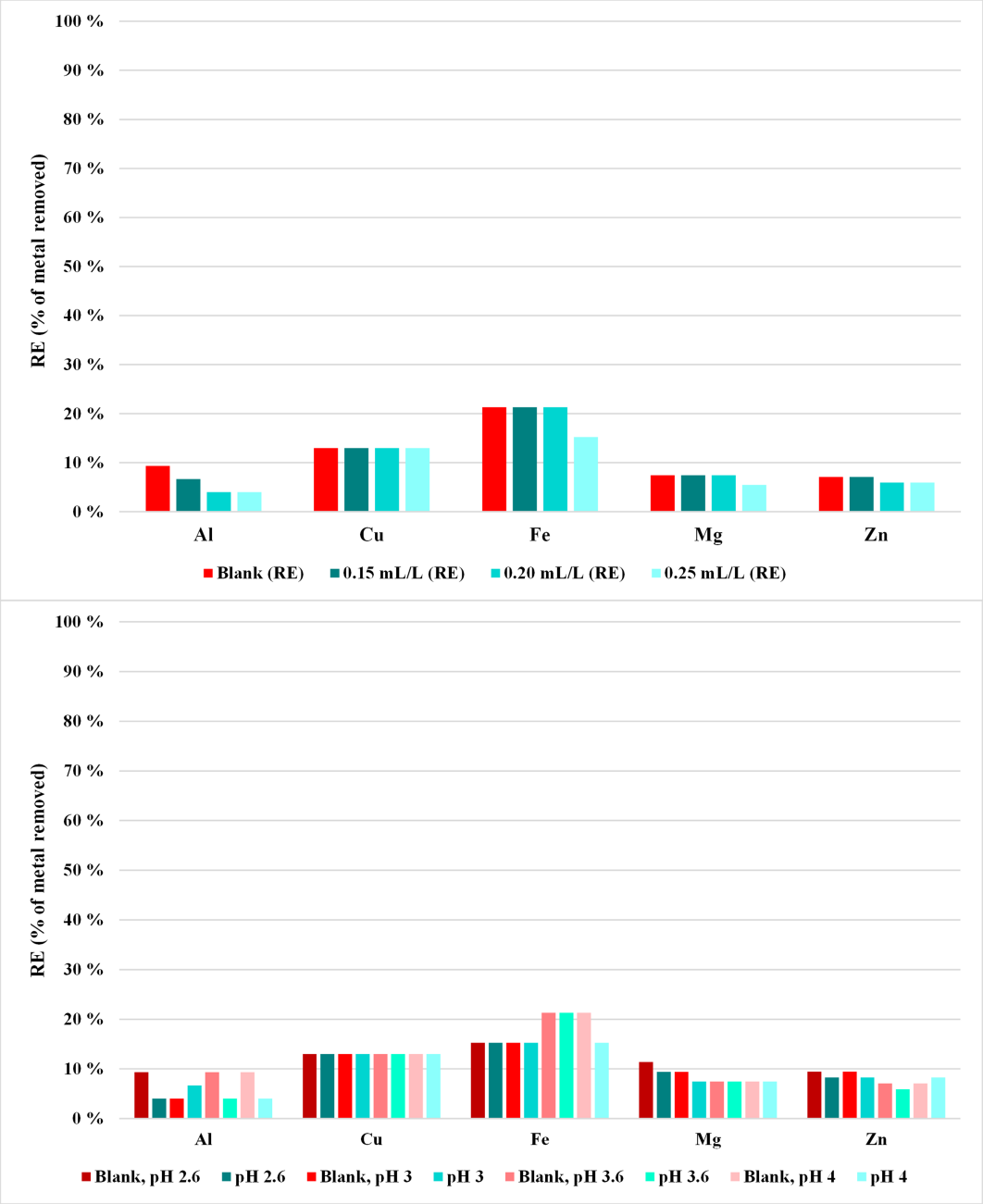

Figure E.1: Diagrams showing the performance of chitosan as primary coagulant with different doses and pH.

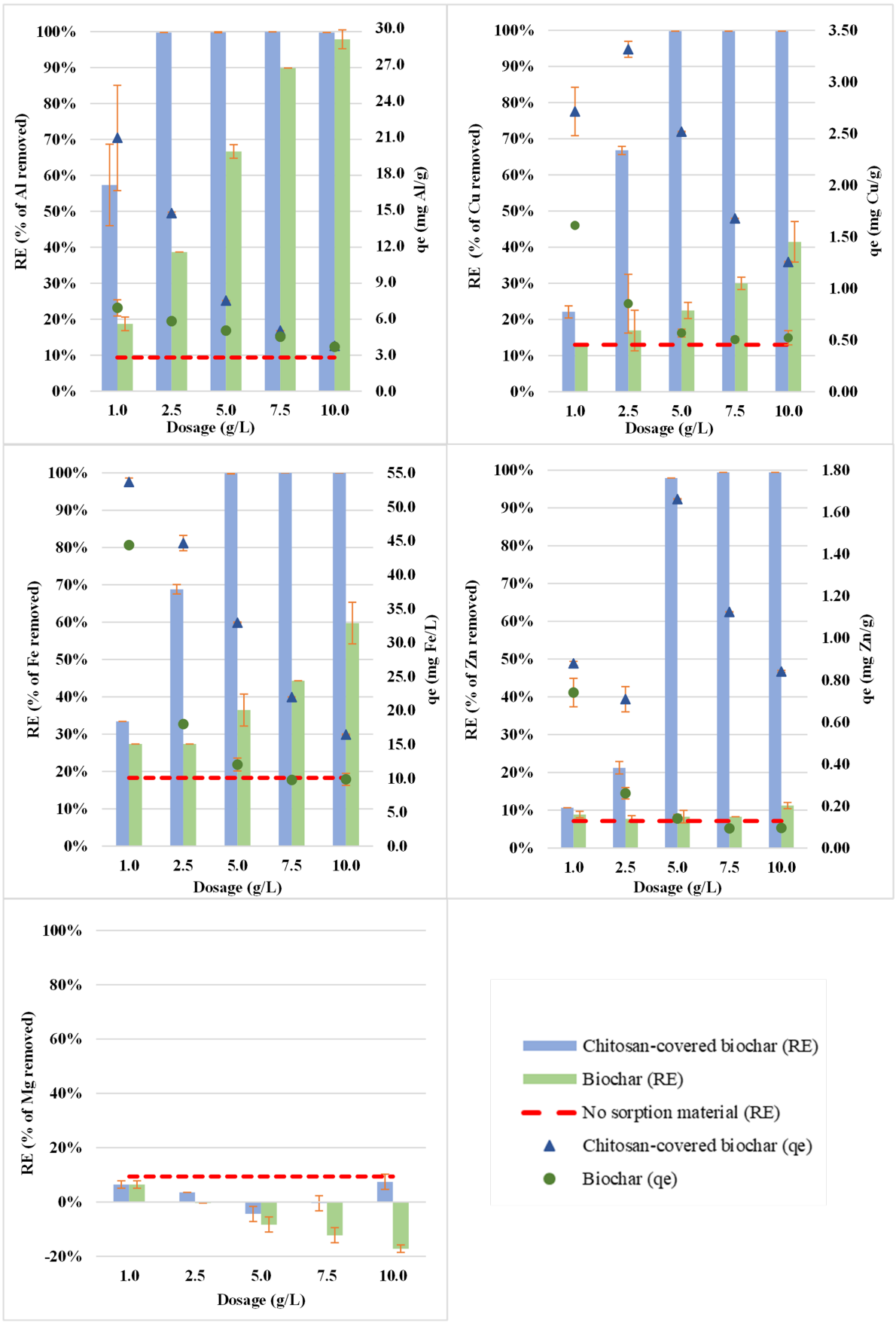

Figure E.2: Diagrams of results with different dosages.

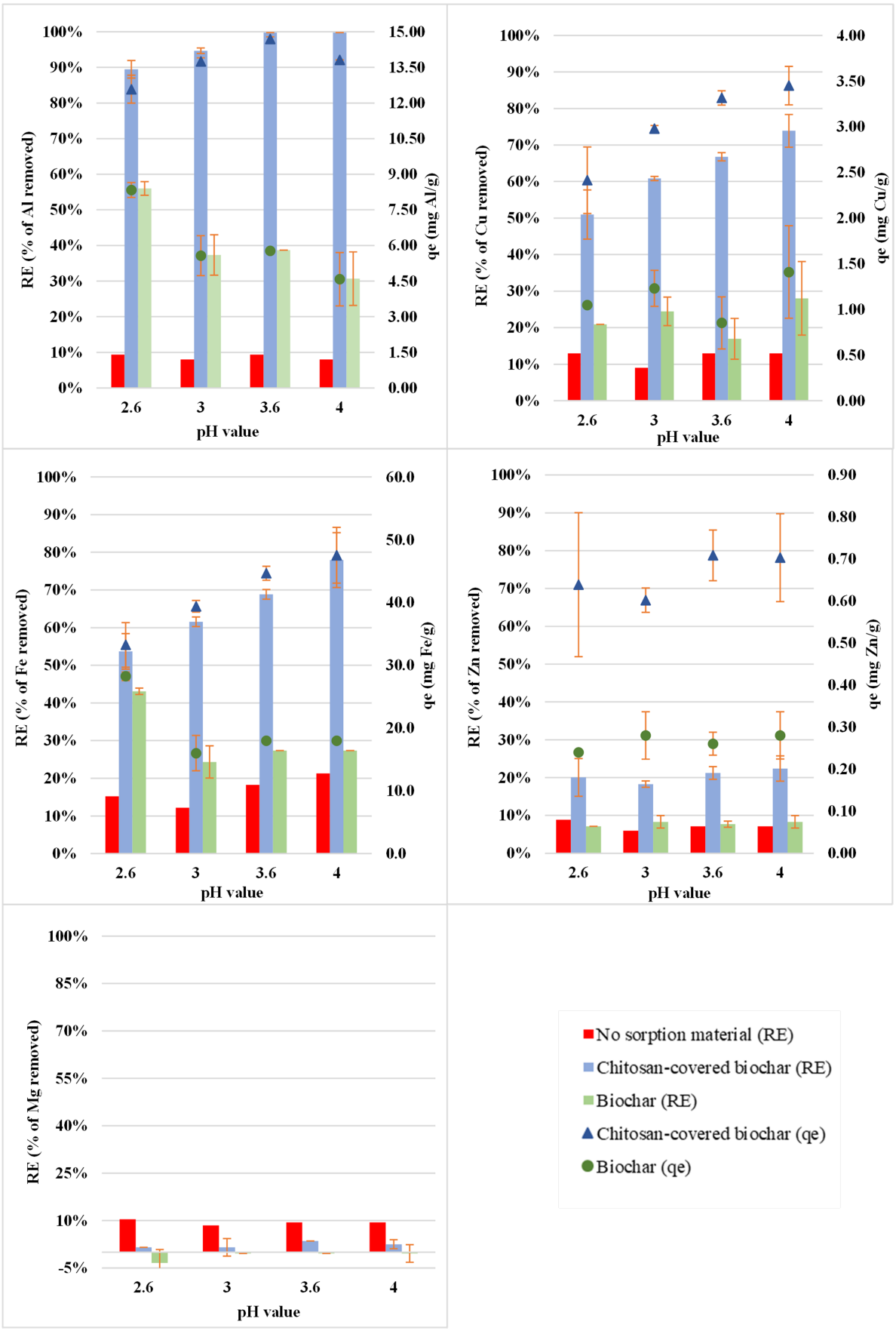

Figure E.3: Diagrams of results with different pH.

Appendix F. Results in tables

Table F.1: The concentration of the metals in the AMD collected 07.02.22.

Element	**Concentration (μg/L)**
Al	37500 ± 1291
Ca	3350 ± 370
Cd	26 ± 1.6
Cr	86 ± 3.0
Cu	12500 ± 577
Fe	165000 ± 17321
Mg	50750 ± 1708
Mn	1325 ± 50
Ni	115 ± 5.9
Pb	<10 ± 0
Zn	8250 ± 500
Ba	13 ± 2.2
Co	283 ± 13
Sr	40 ± 1.59
V	16 ± 0.67
Temperature	3.3°C
pH	2.95
Conductivity	3.82 mS/cm
TSS	160 ± 43 mg TSS/L
TDS	6213 ± 46 mg TDS/L

Model water made is based on the underlined elements.

Table F.2: Results for adsorption batch tests performed on synthetic water.

pH	Material (dose)	Al (µg/L)		Cu (µg/L)		Fe (µg/L)		Mg (µg/L)		Zn (µg/L)	
		C_i	C_f	C_i	C_f	C_i	C_f	C_i	C_f	C_i	C_f
3.6	**MB**	37504	34000 ± 1414	12641	11000 ± 0	165179	135000 ± 7071	50785	46000 ± 1414	8505	7900 ± 141
	B (0.200g)	37504	<800 ± 990	12641	7400 ± 707	165179	66500 ± 9192	50785	59500 ± 707	8505	7550 ± 71
	CH-B (0.200g)	37504	<100 ± 0	12641	<30 ± 0	165179	<9 ± 0	50785	47000 ± 1414	8505	<50 ± 0
	B (0.150g)	37504	3800 ± 0	12641	8850 ± 212	165179	92000 ± 0	50785	57000 ± 1414	8505	7800 ± 0
	CH-B (0.150g)	37504	<30 ± 0	12641	<30 ± 0	165179	<9 ± 0	50785	51000 ± 1414	8505	<50 ± 0
	B (0.100g)	37504	12500 ± 707	12641	9800 ± 283	165179	105000 ± 7071	50785	55000 ± 1414	8505	7800 ± 141
	CH-B (0.100g)	37504	<65 ± 49	12641	<30 ± 0	165179	<180 ± 241	50785	53000 ± 1414	8505	<180 ± 0
	B (0.050g)	37504	23000 ± 0	12641	10500 ± 707	165179	120000 ± 0	50785	51000 ± 0	8505	7850 ± 71
	CH-B (0.050g)	37504	<100 ± 0	12641	4200 ± 141	165179	51500 ± 2121	50785	49000 ± 0	8505	6700 ± 141
	B (0.020g)	37504	30500 ± 707	12641	11000 ± 0	165179	120000 ± 0	50785	47500 ± 707	8505	7750 ± 71
	CH-B (0.020g)	37504	16000 ± 4243	12641	9850 ± 212	165179	110000 ± 0	50785	47500 ± 707	8505	7600 ± 0
2.6	**MB**	37504	34500 ± 707	12641	11000 ± 0	165179	140000 ± 0	50785	45500 ± 707	8505	7700 ± 0
	B (0.050g)	37504	16500 ± 707	12641	10000 ± 0	165179	94000 ± 1414	50785	52500 ± 2121	8505	7900 ± 0
	CH-B (0.050g)	37504	3950 ± 919	12641	6200 ± 849	165179	76500 ± 7778	50785	50000 ± 0	8505	6800 ± 424
3	**MB**	37504	36000 ± 0	12641	11500 ± 707	165179	145000 ± 7071	50785	46500 ± 707	8505	7950 ± 354
	B (0.050g)	37504	23500 ± 2121	12641	9550 ± 495	165179	125000 ± 7071	50785	51000 ± 0	8505	7800 ± 141
	CH-B (0.050g)	37504	2000 ± 283	12641	4950 ± 71	165179	63500 ± 2121	50785	50000 ± 1414	8505	6950 ± 71
4	**MB**	37504	34500 ± 707	12641	11000 ± 0	165179	130000 ± 0	50785	45000 ± 1414	8505	7900 ± 0
	B (0.050g)	37504	26000 ± 2828	12641	9100 ± 1273	165179	120000 ± 0	50785	51000 ± 1414	8505	7800 ± 141
	CH-B (0.050g)	37504	<100 ± 0	12641	3300 ± 566	165179	36500 ± 12021	50785	49500 ± 707	8505	6600 ± 283

Results marked with '>' indicates results below limit of quantification and limit of detection
Abbreviations: C_i, initial concentration; C_f, final concentration; MB, matrix blank; B, biochar; CH-B, chitosan-covered biochar.

Table F.3: The concentration of metals in the sample of the AMD collected 02.05.2022.

Element	**Concentration (µg/L)**
Al	160000 ± 0
Ca	200000 ± 0
Cd	110 ± 0
Cr	373 ± 5.8
Cu	43667 ± 1155
Fe	800000 ± 10000
Mg	200000 ± 0
Mn	5967 ± 58
Ni	423 ± 15.3
Zn	38000 ± 0
Temperature	3.2°C
pH	3.6
Conductivity	4.46 mS/cm
Turbidity	23.5 FNU

Model water made is based on the underlined elements.

Table F.4: Result from last adsorption batch test with AMD.

Element	Material (dose):	MB (no material)	B (10.0 g/L)	CH-B (5.0 g/L)
	C_i (µg/L)	**$C_{f,MB}$ (µg/L)**	**$C_{f,B}$ (µg/L)**	**$C_{f,CH-B}$ (µg/L)**
Al	160000 ± 0	153333 ± 5164	150000 ± 0	203333 ± 5774
Ca	200000 ± 0	190000 ± 0	516667 ± 40415	256667 ± 5774
Cd	110 ± 0	110 ± 0	110 ± 0	110 ± 0
Cr	373 ± 5.8	325 ± 24	207 ± 55	173 ± 29
Cu	43667 ± 1155	42667 ± 1033	43000 ± 0	43333 ± 577
Fe	800000 ± 10000	485000 ± 102127	79000 ± 47508	51667 ± 14295
Mg	200000 ± 0	191667 ± 4082	236667 ± 5774	210000 ± 0
Mn	5967 ± 58	5700 ± 63	7333 ± 58	6267 ± 58
Ni	423 ± 15.3	428 ± 12	433 ± 6	417 ± 12
Zn	38000 ± 0	37667 ± 516	40000 ± 0	37667 ± 577

Abbreviations: MB, matrix blank; B, biochar; CH-B, chitosan-covered biochar; C_i, initial concentration of metal; $C_{f,X}$, final concentration of metals after adsorption batch test with(out any) material X.

Table F.5: Results from the experiments with Kitoflokk^{TM} 100 as flocculant aid.

Dose of added Kitoflokk^{TM} 100	**Concentration of metals (µg/L)**											
	Al	Ca	Cd	Cr	Cu	Fe	Mg	Mn	Ni	Zn	**pH$_f$**	**Cond$_f$ (mS/cm)**
0 (MB)	<34	165000 ± 12910	<0.042	<0.17	<2.7	<48	83500 ± 14341	<4.5	<0.085	<9.6	8.54 ± 0.31	23.97 ± 0.06
0.35 (mL/L)	<34	155000 ± 12910	<0.042	<0.17	<2.7	<48	91750 ± 33160	<4.5	<0.085	<9.6	8.26 ± 0.16	23.90 ± 0.00
0.40 (mL/L)	<34	147500 ± 5000	<0.042	<0.17	<2.7	<48	91750 ± 21077	<4.5	<0.085	<9.6	8.20 ± 0.26	23.90 ± 0.26
0.45 (mL/L)	<34	147500 ± 5000	<0.042	<0.17	<2.7	<48	84250 ± 18191	<4.5	<0.085	<9.6	8.10 ± 0.15	23.57 ± 0.67
0.50 (mL/L)	<34	143333 ± 20817	<0.042	<0.17	<2.7	<48	80000 ± 33407	<4.5	<0.085	<9.6	7.50 ± 0.45	23.83 ± 0.15
0.55 (mL/L)	<34	143333 ± 20817	<0.042	<0.17	<2.7	<48	89000 ± 18193	<4.5	<0.085	<9.6	7.64 ± 0.47	24.00 ± 0.06

Abbreviations: pH$_f$, final pH value after jar test; Cond$_f$, final conductivity after jar test; MB, matrix blank.

Appendix G. Calibration Report ICP-MS

Calibration for 004CALS.d

Batch Folder: D:\Data\20220524 Noor_jartest3.b\
Analysis File: 20220524 Noor_jartest3.batch.bin
DA Date-Time: 6/10/2022 1:28:46 PM
Calibration Title:
Calibration Method: External Calibration
VIS Interpolation Fit:

Level	Standard Data File	Sample Name	Acq. Date-Time
1	002CALB.d	Cal Blank	5/25/2022 10:17:08 AM
2	003CALS.d	Std1	5/25/2022 10:19:36 AM
3	004CALS.d	Std2	5/25/2022 10:22:04 AM
4			
5			
6			
7			

Calibration for 004CALS.d

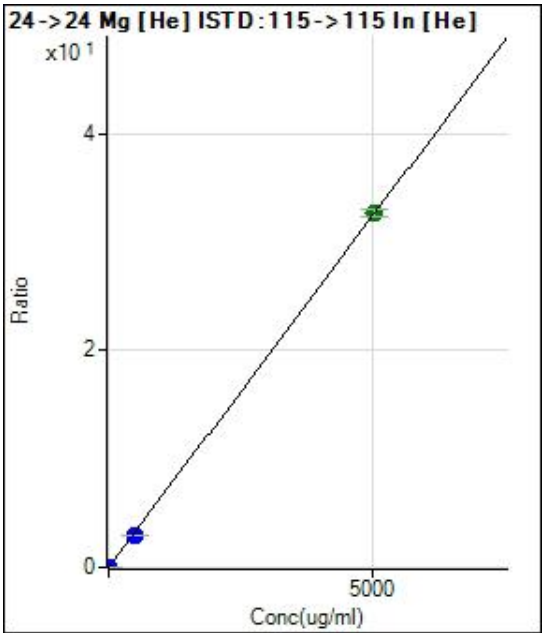

	Rjct	Conc.	Calc Conc.	CPS	Ratio	Det.	RSD
1	☐	0.000	0.000	368.89	0.0081	P	13.0
2	☐	502.000	450.887	132093.35	2.9349	P	2.1
3	☐	5020.000	5025.111	1413935.01	32.6267	A	2.0
4	☐						
5	☐						
6	☐						
7	☐						

y = 0.0065 * x + 0.0081
R = 1.0000
DL = 0.4878
BEC = 1.255

Weight: <None>
Min Conc: 0

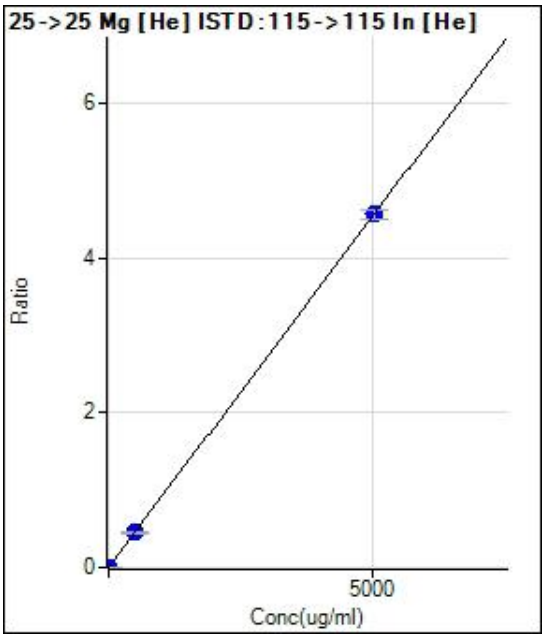

	Rjct	Conc.	Calc Conc.	CPS	Ratio	Det.	RSD
1	☐	0.000	0.000	32.22	0.0007	P	42.8
2	☐	502.000	499.020	20466.84	0.4548	P	3.7
3	☐	5020.000	5020.298	197876.50	4.5689	P	2.6
4	☐						
5	☐						
6	☐						
7	☐						

y = 9.0995E-004 * x + 7.1396E-004
R = 1.0000
DL = 1.007
BEC = 0.7846

Weight: <None>
Min Conc: 0

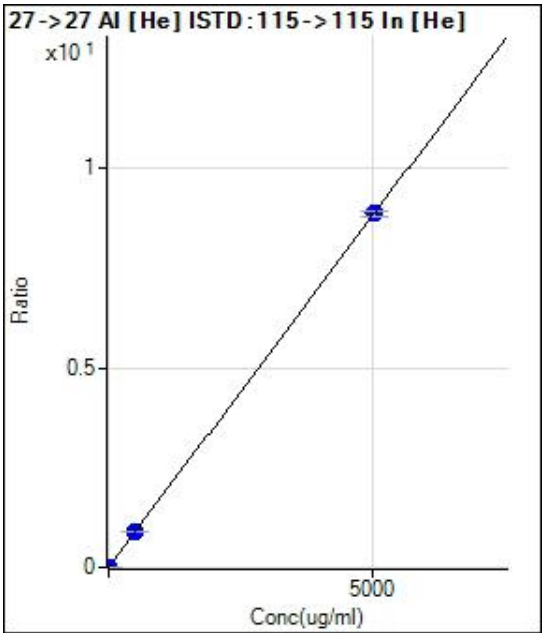

	Rjct	Conc.	Calc Conc.	CPS	Ratio	Det.	RSD
1	☐	0.000	0.000	84.44	0.0019	P	7.0
2	☐	502.000	501.196	39921.75	0.8870	P	2.1
3	☐	5020.000	5020.080	384099.58	8.8678	P	1.6
4	☐						
5	☐						
6	☐						
7	☐						

y = 0.0018 * x + 0.0019
R = 1.0000
DL = 0.2228
BEC = 1.057

Weight: <None>
Min Conc: 0

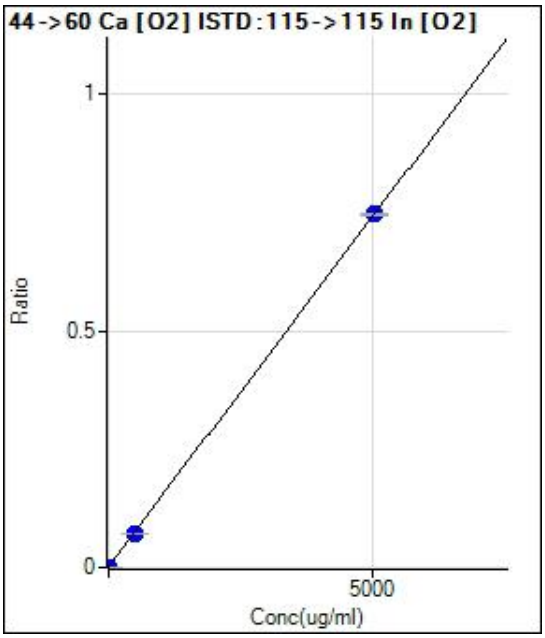

	Rjct	Conc.	Calc Conc.	CPS	Ratio	Det.	RSD
1	☐	0.000	0.000	376.67	0.0014	P	10.0
2	☐	502.000	480.544	18948.80	0.0727	P	1.0
3	☐	5020.000	5022.146	187612.24	0.7465	P	0.7
4	☐						
5	☐						
6	☐						
7	☐						

y = 1.4835E-004 * x + 0.0014
R = 1.0000
DL = 2.929
BEC = 9.76

Weight: <None>
Min Conc: 0

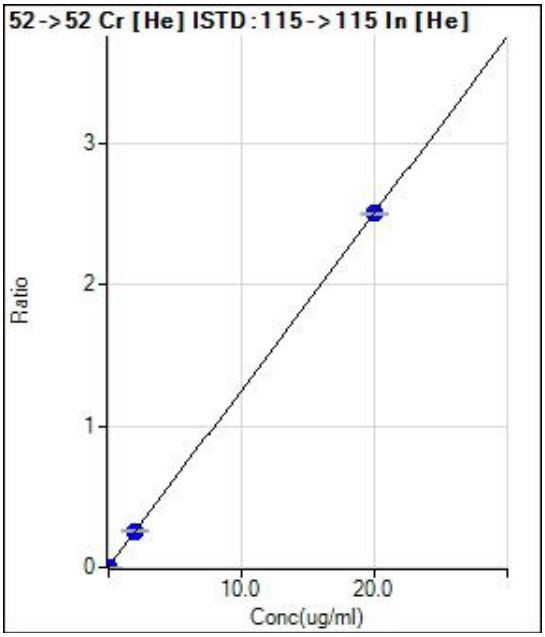

	Rjct	Conc.	Calc Conc.	CPS	Ratio	Det.	RSD
1	☐	0.000	0.000	135.55	0.0030	P	7.0
2	☐	2.000	2.043	11608.16	0.2580	P	4.7
3	☐	20.000	19.996	108258.42	2.4990	P	0.7
4	☐						
5	☐						
6	☐						
7	☐						

y = 0.1248 * x + 0.0030
R = 1.0000
DL = 0.005015
BEC = 0.02398

Weight: <None>
Min Conc: 0

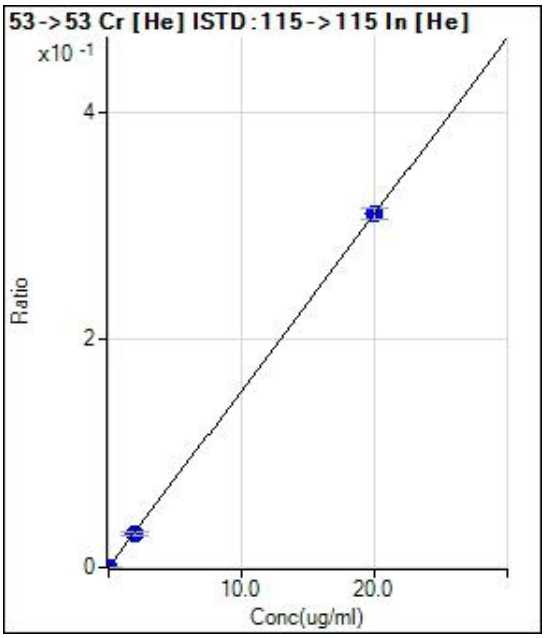

	Rjct	Conc.	Calc Conc.	CPS	Ratio	Det.	RSD
1	☐	0.000	0.000	8.89	0.0002	P	77.5
2	☐	2.000	1.938	1358.94	0.0302	P	12.0
3	☐	20.000	20.006	13428.29	0.3101	P	3.1
4	☐						
5	☐						
6	☐						
7	☐						

y = 0.0155 * x + 1.9560E-004
R = 1.0000
DL = 0.02935
BEC = 0.01263

Weight: <None>
Min Conc: 0

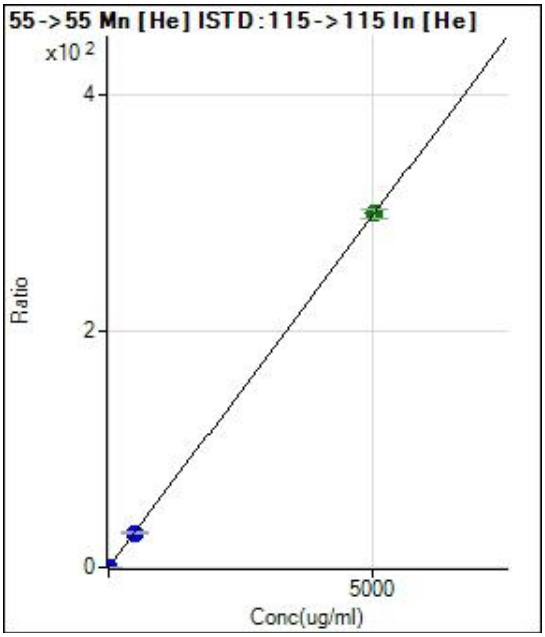

	Rjct	Conc.	Calc Conc.	CPS	Ratio	Det.	RSD
1	☐	0.000	0.000	316.67	0.0070	P	16.8
2	☐	502.000	489.872	1316374.95	29.2476	P	1.6
3	☐	5020.000	5021.213	12980704.49	299.7249	A	2.8
4	☐						
5	☐						
6	☐						
7	☐						

y = 0.0597 * x + 0.0070
R = 1.0000
DL = 0.05909
BEC = 0.1173

Weight: <None>
Min Conc: 0

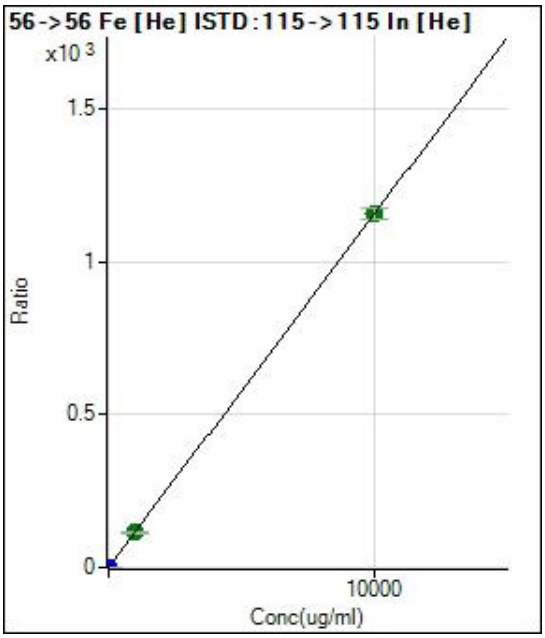

	Rjct	Conc.	Calc Conc.	CPS	Ratio	Det.	RSD
1	☐	0.000	0.000	4116.03	0.0910	P	5.6
2	☐	1002.000	992.945	5157833.96	114.6124	A	3.6
3	☐	10020.000	10020.905	50053415.79	1,155.8534	A	3.3
4	☐						
5	☐						
6	☐						
7	☐						

y = 0.1153 * x + 0.0910
R = 1.0000
DL = 0.132
BEC = 0.7887

Weight: <None>
Min Conc: 0

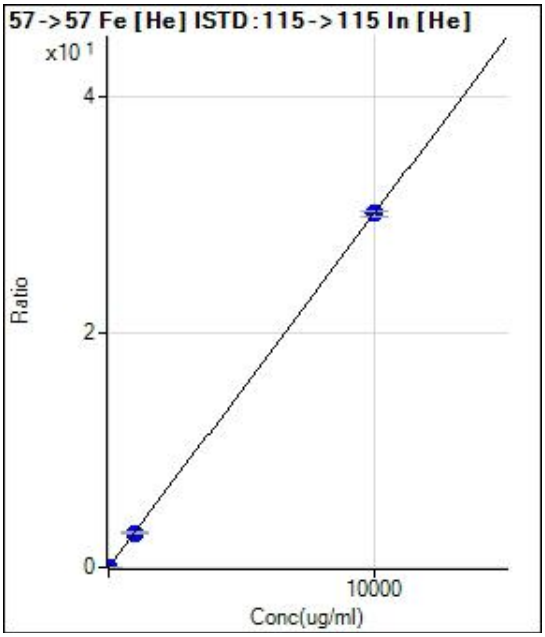

	Rjct	Conc.	Calc Conc.	CPS	Ratio	Det.	RSD
1	☐	0.000	0.000	128.89	0.0029	P	43.7
2	☐	1002.000	973.791	131830.31	2.9289	P	2.0
3	☐	10020.000	10022.821	1304563.73	30.1190	P	1.7
4	☐						
5	☐						
6	☐						
7	☐						

y = 0.0030 * x + 0.0029
R = 1.0000
DL = 1.246
BEC = 0.9501

Weight: <None>
Min Conc: 0

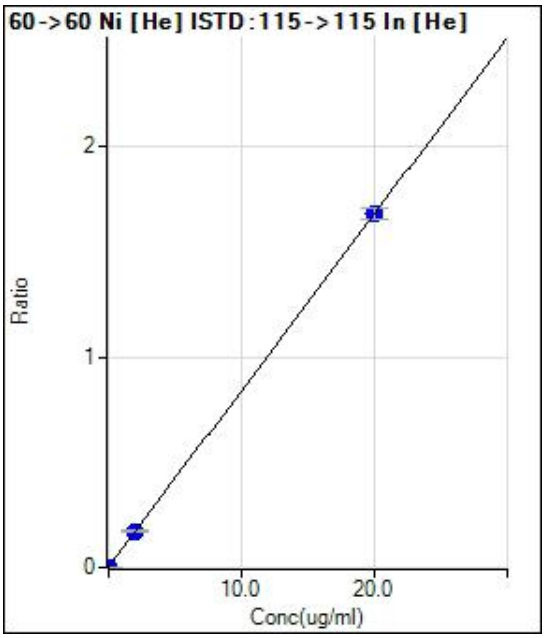

	Rjct	Conc.	Calc Conc.	CPS	Ratio	Det.	RSD
1	☐	0.000	0.000	133.33	0.0030	P	23.7
2	☐	2.000	2.008	7706.11	0.1711	P	5.3
3	☐	20.000	19.999	72656.61	1.6778	P	3.3
4	☐						
5	☐						
6	☐						
7	☐						

y = 0.0837 * x + 0.0030
R = 1.0000
DL = 0.02509
BEC = 0.03523

Weight: <None>
Min Conc: 0

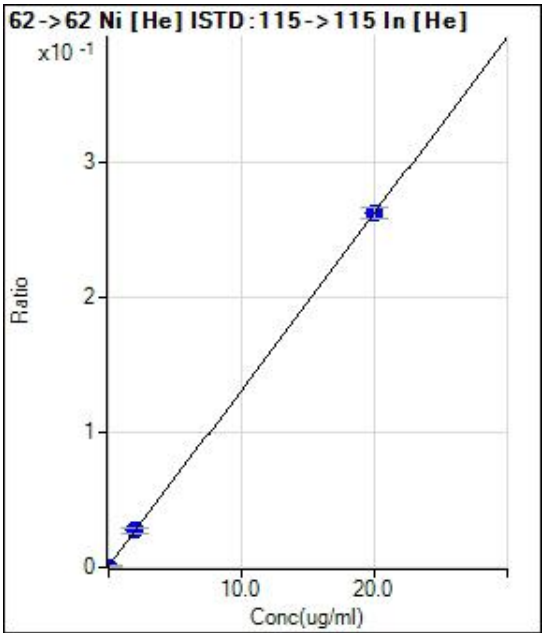

	Rjct	Conc.	Calc Conc.	CPS	Ratio	Det.	RSD
1	☐	0.000	0.000	31.11	0.0007	P	37.1
2	☐	2.000	2.040	1231.15	0.0273	P	13.1
3	☐	20.000	19.996	11343.58	0.2619	P	3.1
4	☐						
5	☐						
6	☐						
7	☐						

y = 0.0131 * x + 6.8630E-004
R = 1.0000
DL = 0.05854
BEC = 0.05253

Weight: <None>
Min Conc: 0

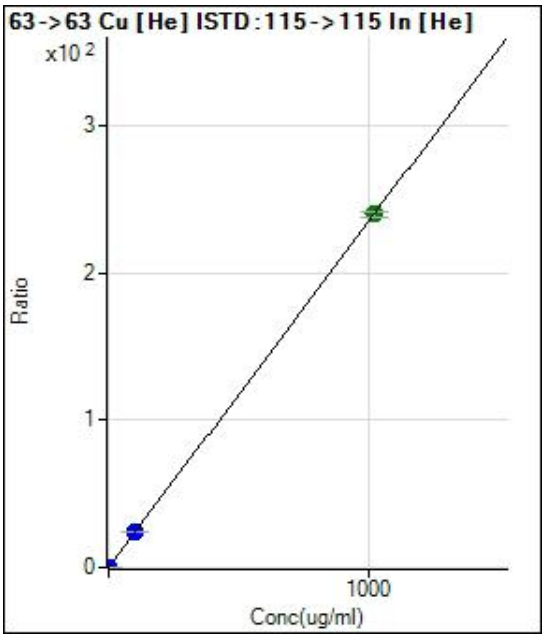

	Rjct	Conc.	Calc Conc.	CPS	Ratio	Det.	RSD
1	☐	0.000	0.000	1157.82	0.0256	P	2.7
2	☐	102.000	104.370	1108068.12	24.6147	P	1.2
3	☐	1020.000	1019.763	10407431.25	240.2767	A	1.6
4	☐						
5	☐						
6	☐						
7	☐						

y = 0.2356 * x + 0.0256
R = 1.0000
DL = 0.008687
BEC = 0.1086

Weight: <None>
Min Conc: 0

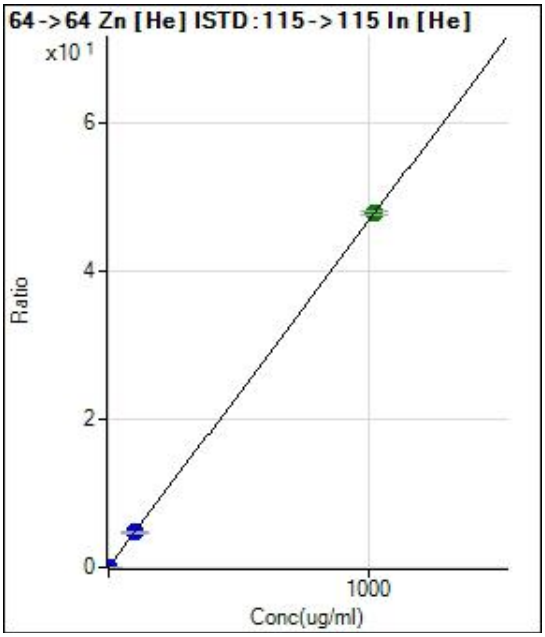

	Rjct	Conc.	Calc Conc.	CPS	Ratio	Det.	RSD
1	☐	0.000	0.000	1284.23	0.0284	P	6.8
2	☐	102.000	100.056	211833.91	4.7056	P	1.5
3	☐	1020.000	1020.194	2067087.57	47.7188	A	1.2
4	☐						
5	☐						
6	☐						
7	☐						

y = 0.0467 * x + 0.0284
R = 1.0000
DL = 0.1238
BEC = 0.607

Weight: <None>
Min Conc: 0

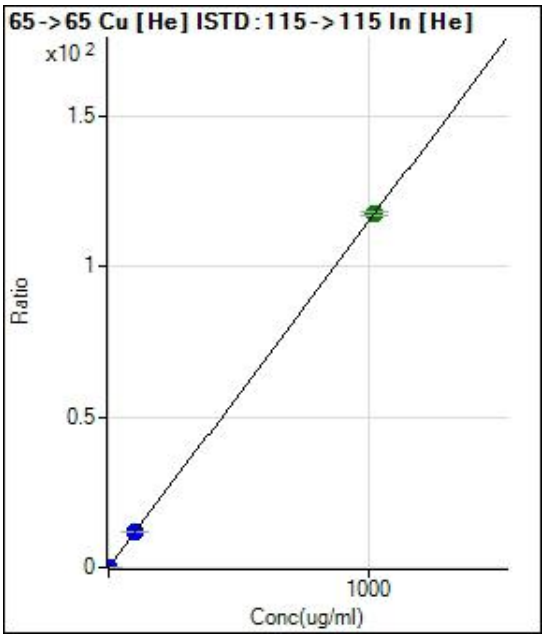

	Rjct	Conc.	Calc Conc.	CPS	Ratio	Det.	RSD
1	☐	0.000	0.000	574.45	0.0127	P	4.3
2	☐	102.000	103.617	537866.68	11.9485	P	0.8
3	☐	1020.000	1019.838	5089951.74	117.4899	A	1.1
4	☐						
5	☐						
6	☐						
7	☐						

y = 0.1152 * x + 0.0127
R = 1.0000
DL = 0.0141
BEC = 0.1102

Weight: <None>
Min Conc: 0

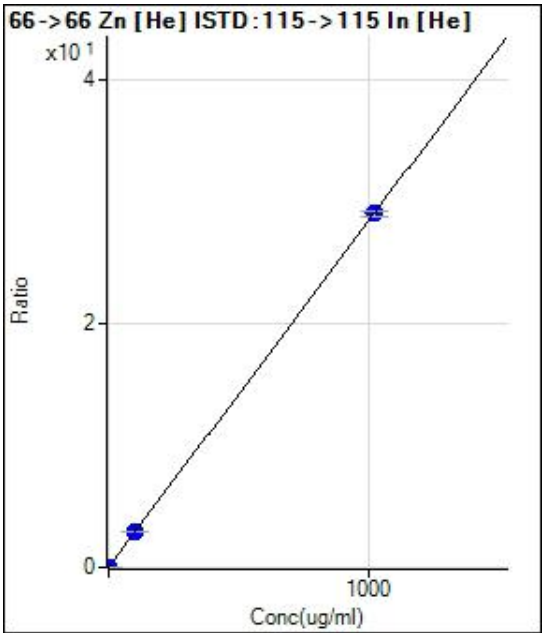

	Rjct	Conc.	Calc Conc.	CPS	Ratio	Det.	RSD
1	☐	0.000	0.000	734.46	0.0162	P	2.8
2	☐	102.000	103.256	133170.29	2.9585	P	0.1
3	☐	1020.000	1019.874	1259629.67	29.0776	P	1.4
4	☐						
5	☐						
6	☐						
7	☐						

y = 0.0285 * x + 0.0162
R = 1.0000
DL = 0.04813
BEC = 0.5694

Weight: <None>
Min Conc: 0

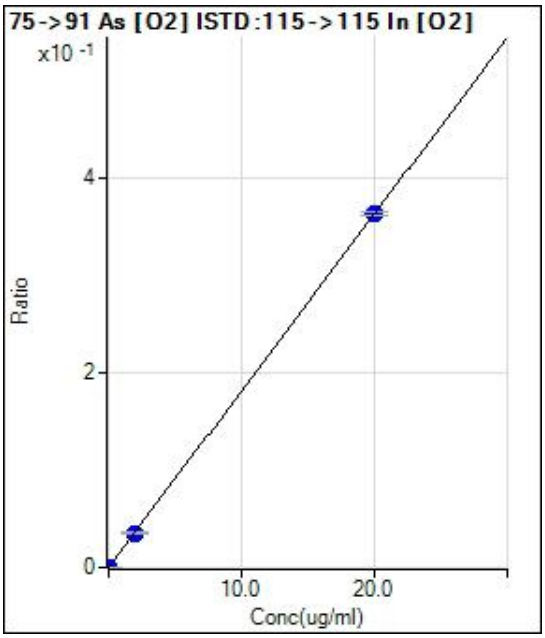

	Rjct	Conc.	Calc Conc.	CPS	Ratio	Det.	RSD
1	☐	0.000	0.000	25.56	0.0001	P	30.7
2	☐	2.000	1.952	9237.99	0.0355	P	3.0
3	☐	20.000	20.005	91132.61	0.3626	P	0.9
4	☐						
5	☐						
6	☐						
7	☐						

y = 0.0181 * x + 9.8391E-005
R = 1.0000
DL = 0.005003
BEC = 0.005429

Weight: <None>
Min Conc: 0

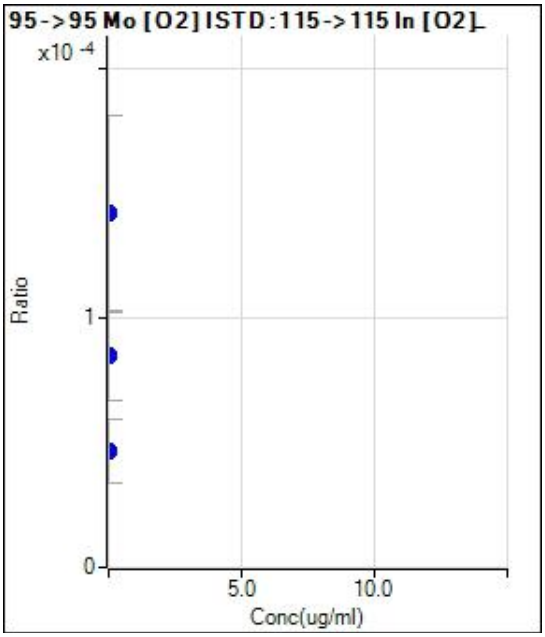

	Rjct	Conc.	Calc Conc.	CPS	Ratio	Det.	RSD
1	☐	0.000		22.22	0.0001	P	42.4
2	☐	0.000		12.22	0.0000	P	55.5
3	☐	0.000		35.55	0.0001	P	55.5
4	☐						
5	☐						
6	☐						
7	☐						

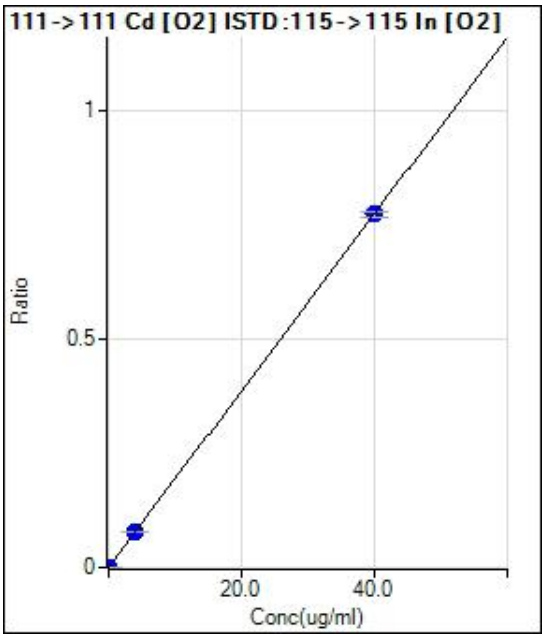

	Rjct	Conc.	Calc Conc.	CPS	Ratio	Det.	RSD
1	☐	0.000	0.000	8.89	0.0000	P	77.3
2	☐	4.000	4.014	20255.16	0.0778	P	3.9
3	☐	40.000	39.999	194660.47	0.7747	P	1.8
4	☐						
5	☐						
6	☐						
7	☐						

y = 0.0194 * x + 3.4055E-005
R = 1.0000
DL = 0.004077
BEC = 0.001758

Weight: <None>
Min Conc: 0

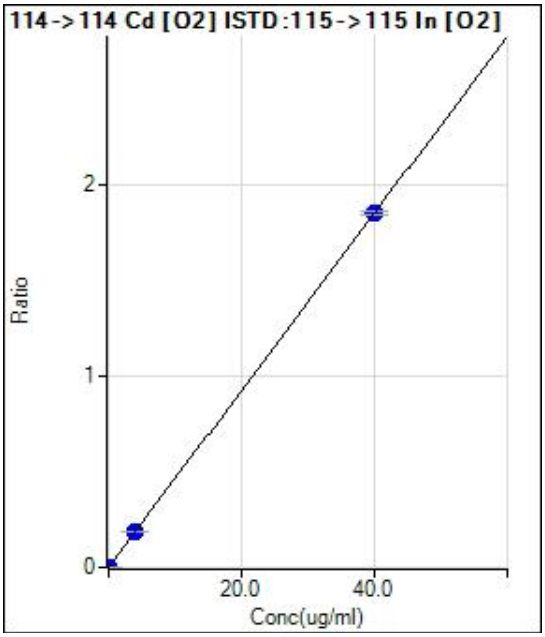

	Rjct	Conc.	Calc Conc.	CPS	Ratio	Det.	RSD
1	☐	0.000	0.000	11.69	0.0000	P	78.8
2	☐	4.000	4.007	48312.83	0.1855	P	2.3
3	☐	40.000	39.999	465184.93	1.8511	P	1.0
4	☐						
5	☐						
6	☐						
7	☐						

y = 0.0463 * x + 4.4901E-005
R = 1.0000
DL = 0.002295
BEC = 0.0009702

Weight: <None>
Min Conc: 0

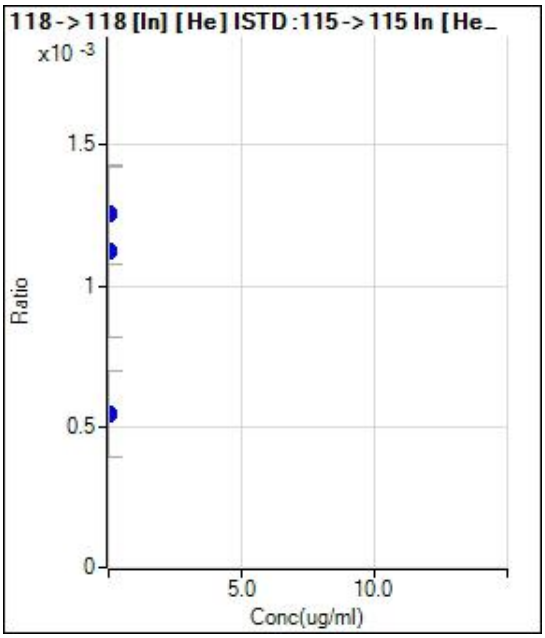

	Rjct	Conc.	Calc Conc.	CPS	Ratio	Det.	RSD
1	☐	0.000		56.67	0.0013	P	27.8
2	☐	0.000		24.45	0.0005	P	55.8
3	☐	0.000		48.89	0.0011	P	53.5
4	☐						
5	☐						
6	☐						
7	☐						

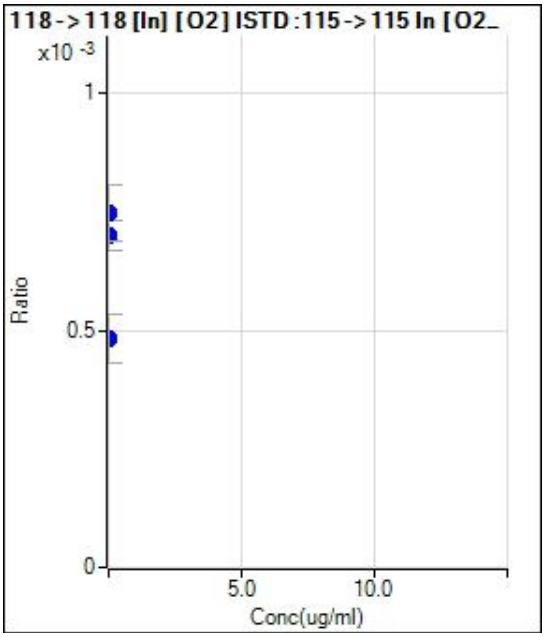

	Rjct	Conc.	Calc Conc.	CPS	Ratio	Det.	RSD
1	☐	0.000		182.22	0.0007	P	8.9
2	☐	0.000		125.55	0.0005	P	21.1
3	☐	0.000		187.78	0.0007	P	15.9
4	☐						
5	☐						
6	☐						
7	☐						

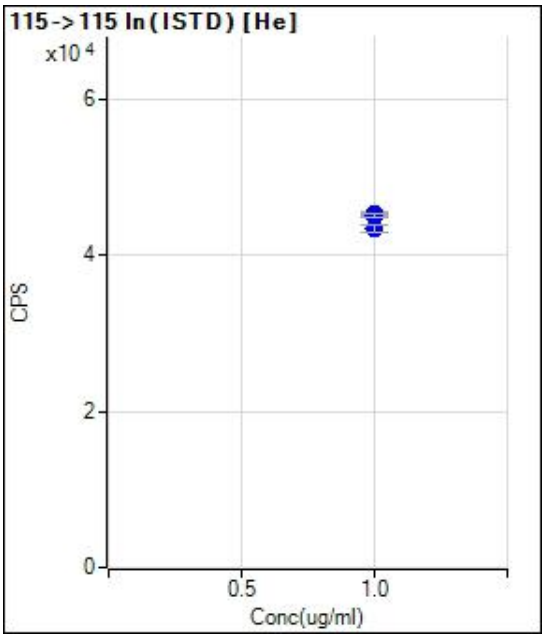

	Rjct	Conc.	Calc Conc.	CPS	Ratio	Det.	RSD
1	☐	1.000		45257.88		P	1.0
2	☐	1.000		45012.80		P	1.0
3	☐	1.000		43324.07		P	2.2
4	☐	1.000					
5	☐	1.000					
6	☐	1.000					
7	☐	1.000					

Calibration for 004CALS.d

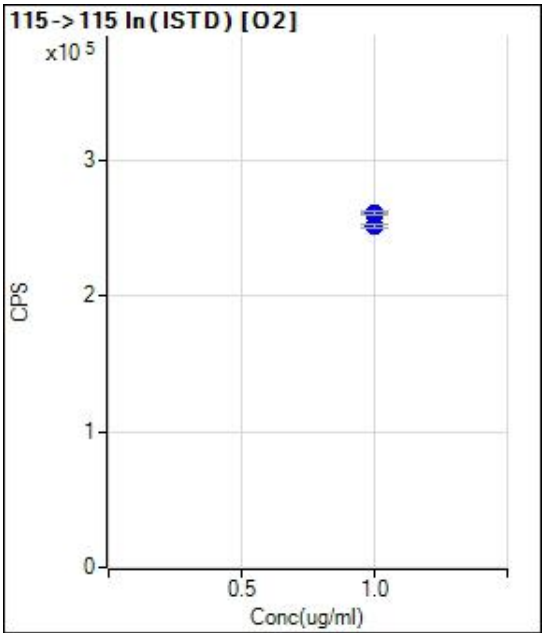

	Rjct	Conc.	Calc Conc.	CPS	Ratio	Det.	RSD
1	☐	1.000		260168.59		P	0.9
2	☐	1.000		260518.59		P	1.2
3	☐	1.000		251314.57		P	1.2
4	☐	1.000					
5	☐	1.000					
6	☐	1.000					
7	☐	1.000					

Norges miljø- og biovitenskapelige universitet
Noregs miljø- og biovitskapelege universitet
Norwegian University of Life Sciences

Postboks 5003
NO-1432 Ås
Norway